Combined Hyperglycemia and Hyperinsulinemia-induced Insulin Resistance in Adipocytes is associated with Dual Signaling Defects mediated by PKC-

Lu, Huogen; Bogdanovic, Elena; Yu, Zhiwen; Cho, Charles; Liu, Lijiang; Ho, Karen; Guo, June; Yeung, Lucy S. N.; Lehmann, Reiner; Hundal, Harinder S.; Giacca, Adria; Fantus, I. George

Published in:
Endocrinology

DOI:
10.1210/en.2017-00312

Publication date:
2018

Document Version
Peer reviewed version

Combined Hyperglycemia and Hyperinsulinemia-induced Insulin Resistance in Adipocytes is associated with Dual Signaling Defects mediated by PKC-ζ

Huogen Lu, Elena Bogdanovic, Zhiwen Yu, Charles Cho, Lijiang Liu, Karen Ho, June Guo, Lucy SN Yeung, Reiner Lehmann, Harinder S. Hundal, Adria Giacca and I. George Fantus

Endocrinology
Endocrine Society

Submitted: March 31, 2017
Accepted: January 03, 2018
First Online: January 23, 2018

Endocrinology; Copyright 2018 DOI: 10.1210/en.2017-00312

PKC-ζ and Insulin Resistance

Combined Hyperglycemia and Hyperinsulinemia-induced Insulin Resistance in Adipocytes is associated with Dual Signaling Defects mediated by PKC-ζ

Huogen Lu[1,3], Elena Bogdanovic[1,2,3], Zhiwen Yu[1,3], Charles Cho[1,2], Lijiang Liu[1,3], Karen Ho[1,3], June Guo[2], Lucy SN Yeung[2], Reiner Lehmann[4], Harinder S. Hundal[5], Adria Giacca[2] and I. George Fantus[1,2,3,*]

Departments of Medicine[1] Mount Sinai Hospital, Department of Physiology[2], Banting and Best Diabetes Centre and Toronto General Research Institute[3], University Health Network, University of Toronto, Toronto, ON., Canada, The Department of Internal Medicine IV, Endocrinology, Metabolism, Pathobiochemistry and Clinical Chemistry, University Hospital Tuebingen, D-72076 Tuebingen, Germany[4] and Division of Molecular Physiology Unit, Faculty of Life Sciences, University of Dundee, Dundee DD15EH, United Kingdom[5]

Received 31 March 2017. Accepted 03 January 2018.

1. The abbreviations used are: GLUT, glucose transporter; IRS-1, insulin receptor substrate-1; GSK, glycogen synthase kinase; PKB, protein kinase B; PI, phosphatidylinositol; SH2, Src homology 2; PM, plasma membrane; LDM, low density microsomes; mTORC2, mammalian target of rapamycin-rictor complex 2; PKC, protein kinase C; PS, pseudosubstrate; HG/HG, high glucose/high insulin; 2DG, 2-deoxyglucose; DMEM, Dulbecco's modified Eagles medium; FBS, fetal bovine serum; KRBH, Krebs Ringer Bicarbonate HEPES; TES, Tris EDTA sucrose; PMSF, phenylmethylsulfonide fluoride; HA, hemagglutinin; GFP, green fluorescent protein.

A hyperglycemic and hyperinsulinemic environment characteristic of type 2 diabetes causes insulin resistance. In adipocytes, defects in both insulin sensitivity and maximum response of glucose transport have been demonstrated. To investigate the molecular mechanisms, freshly isolated rat adipocytes were incubated in control (5.6 mM glucose, no insulin) and high glucose (20 mM)/high insulin (100 nM) (HG/HI) for 18 h to induce insulin resistance. Insulin resistant adipocytes manifested decreased sensitivity of glucose uptake associated with defects in IRS-1 Tyr phosphorylation, association of p85 subunit of phosphatidylinositol-3-kinase, AktSer473 and Thr308 phosphorylation accompanied by impaired glucose transporter 4 translocation. In contrast, PKC-ζ activity was augmented by chronic HG/HI. Inhibition of PKC-ζ with a specific cell permeable peptide reversed the signalling defects and insulin sensitivity of glucose uptake. Transfection of dominant-negative kinase-inactive PKC-ζ blocked insulin resistance, while constitutively-active PKC-ζ recapitulated the defects. The HG/HI incubation was associated with stimulation of IRS-1Ser318 and AktThr34 phosphorylation, targets of PKC-ζ. Transfection of IRS-1S318A and AktT34A each partially corrected, while combined transfection of both completely normalized insulin signaling. In vivo hyperglycemia/hyperinsulinemia in rats, for 48h similarly resulted in activation of PKC-ζ and increased phosphorylation of IRS-1 Ser318 and AktThr 34. These data indicate that impairment of insulin signaling by chronic HG/HI is mediated by dual defects at IRS-1 and Akt mediated by PKC-ζ.

Chronic activation of PKC-ζ decreases insulin sensitivity of glucose transport in adipocytes exposed to combined hyperglycemia/hyperinsulinemia by phosphorylation of dual targets, IRS-1 and Akt.

Introduction

Peripheral resistance to the action of insulin is a key contributor to the development of type 2 diabetes and is associated with an increased risk of cardiovascular disease (1-3). Several factors contributing to insulin resistance have been identified including increased circulating fuels,

glucose, free fatty acids (FFA) and amino acids (3-5). In the case of glucose, induction of in vivo hyperglycemia by partial pancreatectomy or streptozotocin resulted in the development of whole body insulin resistance which was corrected by normalization of glucose concentrations (6, 7). Rats infused with high glucose for 72 h show impaired insulin-stimulated glucose uptake in vivo and in isolated tissues (8). In an *in vitro* model, chronic exposure (18 h) of primary cultured rat adipocytes to high concentrations of glucose combined with insulin impaired the ability of insulin to acutely stimulate glucose uptake (9). In this model two types of defects, namely, decreased insulin sensitivity (a shift to the right of the insulin dose-response curve) and decreased responsiveness (maximum insulin response), were noted. The molecular mechanisms that account for these changes have not been defined.

Insulin stimulates glucose entry into skeletal muscle and adipose tissue by promoting the translocation of glucose transporters (GLUTs), mainly GLUT4, from intracellular storage sites to the plasma membrane (PM) (10). Insulin binds to the cell surface insulin receptor, activates its intrinsic tyrosine kinase that phosphorylates insulin receptor substrates (IRSs) (reviewed in 2,11). This results in binding and activation of phosphatidylinositol 3-kinase (PI 3-kinase), which catalyzes the formation of 3′phosphorylated lipid products, PI(3,4)P_2 and PI (3,4,5)P_3. (12). These lipids recruit Akt/protein kinase B (PKB) to the PM and activate the enzyme by its phosphorylation on Thr308 by phosphoinositide-dependent kinase-1 (PDK-1) and Ser473 by the rictor/mTOR complex (mTORC2), respectively (12-14). Akt activation leads to GLUT4 translocation and glucose uptake (15,16). In addition to glucose transport, Akt has been implicated in the stimulation of glycogen synthesis, protein synthesis, transcription, and cell survival (16,17).

Atypical protein kinase C-ζ/λ (PKC-ζ) is also activated by insulin in a PI 3-kinase dependent manner (18,19). This Ser/Thr kinase has also been implicated in glucose transport stimulated by insulin in adipocytes and skeletal muscle (19-22). On the other hand, PKC-ζ has also been found to negatively regulate insulin signaling by phosphorylating IRS-1 (23-26). PKC-ζ has also been reported to phosphorylate Akt and inhibit its activation, associated with metabolic conditions (27). However, the role of PKC-ζ and these targets of phosphorylation in the pathogenesis of insulin resistance in adipocytes has not been well documented. The unique challenge of investigating PKC-ζ is due to the fact that knockout or inhibition of atypical PKC blocks insulin-stimulated glucose transport in target tissues, muscle and adipocytes (20,28).

In this study we investigated insulin signaling in primary cultured rat adipocytes rendered insulin resistant by chronic (18 h) incubation with 20 mM glucose and 100 nM insulin (HG/HI). Tyr phosphorylation of IRS-1, its association with the p85 subunit of PI3K and insulin-stimulated Akt activation were impaired. Surprisingly, in contrast, PKC-ζ activity remained abnormally elevated in the basal state and its inhibition was associated with a recovery of the response to insulin. Concomitant with these findings, impaired GLUT4 translocation and decreased sensitivity of glucose transport were normalized by inhibiting PKC-ζ prior to restimulation with insulin. Transfection of adipocytes with IRS-1S318A or with Akt T34A, mutants of IRS-1 and Akt respectively, in which the Ser/Thr residues recognized as phosphorylation targets of PKC-ζ (26,29) were substituted for alanine, partially restored the defects induced by cotransfected CA (constitutively active) –PKC-ζ or by HG/HI, while cotransfection with both IRS-1S318A and AktT34A completely corrected these defects. Furthermore, 48h in vivo combined hyperglycemia/hyperinsulinemia-induced insulin resistance was associated with increased IRS-1 Ser318, Akt Thr 34 and PKC-ζ Thr 410 phosphorylation.

These data indicate that combined hyperglycemia/hyperinsulinemia-induced insulin resistance is due to enhanced PKC-ζ activity which causes dual defects at the level of IRS-1 and Akt.

Materials and Methods

Reagents:

Dulbecco's Modified Eagle's medium (DMEM), fetal bovine serum (FBS), antibiotics, and the PKC-ζ peptide substrate {[Ser^{25}] PKC residues (19-31)} were purchased from Invitrogen. Type 1 collagenase was from Worthington Biochemicals Corp. (Freehold, NJ). The following chemicals were obtained from Sigma, bovine serum albumin (BSA fraction V), phthalic acid dinonyl ester, rotenone, phloretin, microcystin-RR, 2-deoxyglucose (2DG), and all chemicals used for KRBH (Krebs Ringer Bicarbonate HEPES) and KR30H (KR 30 mM HEPES) buffers. L-α-phosphatidylinositol and myristoylated PKC-ζ pseudosubstrate peptide inhibitor (human PKCζ (amino acid residues 113-125)) (PS) were obtained from Biomol. Anti-phosphotyrosine (pY) (4G10) conjugated to agarose, Akt1/PKBα Immunoprecipitation and Kinase Assay Kit, Akt/PKB substrate peptide Crosstide, antibodies against the p85 subunit of PI3-kinase,IRS-1, IRS-1 pSer307, IRS-1 pSer636/639 and agarose-conjugated anti-IRS-1 were obtained from Upstate-Millipore. Anti-pY (PY99), antibodies against PKC-ζ/λ, anti-Akt2/PKB-β,anti-myc and anti-PKCs (-β_1,-δ and -ε) were from Santa Cruz. Phospho-specific antibodies against Akt pSer473, Akt pThr308, GSK-3α/β pSer21/Ser9, PKC-ζ pThr 410 and antibodies against total PKB and PKC-ζ were obtained from Cell Signaling. Antibodies against GSK3α/β and myristoylated PKC-α/β pseudosubstrate peptide inhibitor (PKC-α residues 20-28) were obtained from Calbiochem-Millipore Antibodies against GLUT1 and GLUT4 were a kind gift from Dr. S. Cushman (National Institutes of Health, Bethesda, MD) or from Novus and Calbiochem-Millipore respectively. Antibody against PKB pThr34 was from Abcam Inc. (Cambridge, MA) and anti-HA from COVANCE (Denver, PA) (Suppl. Table 1). 2-deoxy-D-[^{3}H] glucose (30 Ci/mmol) and [γ-^{32}P] ATP (3000 Ci/mmol) were obtained from DuPont-NEN. Nitrocellulose membranes (0.45 μm) for protein transfer were obtained from Schleicher & Schuell (Keene, NH). The enhanced chemiluminescence (ECL) reagent was obtained from Amersham. Human insulin was a gift from Eli Lilly (Indianapolis, IN).

Primary culture of rat adipocytes:

Male Sprague-Dawley rats (Charles River) weighing 200-250 g were sacrificed by exposure to 30% O_2/70% CO_2 followed by 100% CO_2 and cervical dislocation. Animal studies were carried out in accordance with policies and guidelines of the Canadian Council on Animal Care and approved by the University Health Network Animal Care Committee. The epididymal fat pads were removed and adipocytes liberated by collagenase digestion as previously described (30). Freshly isolated adipocytes were incubated (10% lipocrit) for 18 h at 37°C in DMEM containing 25 mM HEPES, 1% penicillin-streptomycin, 0.5% FBS, and 1% BSA. Cells were incubated either in media alone (Control, 5.6 mM glucose), or containing 20 mM glucose and 100 nM insulin (high glucose (HG)/high insulin (HI), Resistant). All incubations were carried out in a humidified atmosphere of 95% air/5% CO_2. For inhibition of PKC-ζ activity, cells were treated with PS for the final 2 h. Following the 18 h incubation, cells were washed twice with KR30H buffer (137 mM NaC1, 5 mM KC1, 1.2 mM KH_2PO_4, 1.2 mM $MgSO_4$, 1.25 mM $CaCl_2$, 30 mM HEPES, 1 mM pyruvate, pH 7.0) containing 3% BSA, and then incubated in the same buffer for 30 min at 37°C to remove all extracellular and receptor bound insulin (9). The cells were then washed twice in KRBH buffer (118 mM NaCl, 5 mM KCl, 1.2 mM $MgSO_4$, 2.5 mM $CaCl_2$, 1.2

mM KH_2PO_4, 5 mM $NaHCO_3$, 30 mM HEPES, 1 mM pyruvate, pH 7.5) containing 3% BSA and then re-suspended in the same buffer for subsequent stimulation with insulin.

2-deoxyglucose uptake assay:
To assess 2-deoxyglucose (2DG) uptake, adipocytes (6 x 10^5 cells/ml final concentration) were incubated in a shaking water bath for 30 min at 37°C in the presence of various concentrations of insulin (0-100 nM) and carried out as described (31).

Subcellular fractionation of rat adipocytes:
Cells stimulated with or without insulin were washed once with TES homogenization buffer (25 mM Tris, pH 7.4, 2 mM EDTA, 0.25 M sucrose, 0.01 mg/ml aprotinin, 0.01 mg/ml leupeptin, 0.1 mM PMSF) equilibrated at 18°C and homogenized. All subsequent steps were performed at 4°C as described (31). The PM and LDM (low density microsomes) fractions (pellet) were resuspended in Buffer A (50 mM Tris, PH7.5, 1 mM EDTA, 1 mM EGTA, 0.5 mM sodium orthovanadate, 0.1% 2-mercaptoethanol, 1% Triton X-100, 50 mM sodium fluoride, 5 mM sodium pyrophosphate, 10 mM sodium glycerophosphate, 0.1 mM PMSF, 1 μM microcystin-RR, 1 μg/ml each of aproptinin, pepstatin, and leupeptin) and stored at –80°C. The purity of the membrane fractions was confirmed by assays of the PM marker, 5'nucleotidase (Sigma) which was 12.5-fold enriched in PM compared with LDM. The purity and protein yields of PM and LDM were similar in control and resistant cells (not shown).

Western blotting:
Adipocytes were solubilized by adding 300 μl of lysis buffer (50 mM Tris-HCl, pH 7.5, 1 mM EDTA, 1 mM EGTA, 0.5 mM sodium orthovanadate, 0.1% 2-mercaptoethanol, 1% Triton X-100, 50 mM sodium fluoride, 5 mM sodium pyrophosphate, 10 mM sodium β-glycerophosphate, 0.1 mM PMSF, 1 μg/ml aprotinin, 1 μg/ml pepstatin, 1μg/ml leupeptin, and 0.1 μg/ml okadaic acid) per ml of cells followed by homogenization. After centrifugation, the fat was removed, and the infranatant was stored at -70°C. Laemmli sample buffer (3x) with 0.006% bromphenol blue was added to equal aliquots of protein (Bradford assay) and boiled for 5 min. For GLUT4 and GLUT1, urea sample buffer was used (6.86 mol/l urea, 4.29% SDS, 43 mM Tris-HCl, and 300 mM dithiothreitol). For immunoprecipitation, 1 mg of whole cell lysates were incubated with 4 μg of antibody at 4°C overnight followed by addition of 30 μl of protein A/G-agarose beads for 2 h or for IRS-1, with agarose-conjugated antibody. The samples were centrifuged, washed and separated by SDS-PAGE. Proteins were transferred onto nitrocellulose membranes, and immunoblotting performed as described (31). Intensities of all phosphoprotein immunoblots were corrected for the relevant total proteins in each experiment.

Enzyme activity assay:
Cells stimulated with or without insulin were washed twice with ice-cold KRBH and lysed as above. Akt was immunoprecipitated and immunocomplexes washed 3 times with lysis buffer containing 0.5 M NaCl, twice with washing buffer (50 mM Tris-HCl, pH 7.5, 0.03% (w/v) Brij-35, 0.1 mM EGTA and 0.1% 2-mercaptoethanol), and once with the Akt kinase assay buffer (20 mM MOPS, pH 7.2, 25 mM sodium β-glycerophosphate, 5 mM EGTA, 1 mM sodium orthovanadate, 1 mM DTT). Immunoprecipitates were incubated in the assay buffer containing γ [^{32}P]-ATP (10 μCi), and 10 μM Protein Kinase A inhibitor peptide (amino acids 6-22 amide, Calbiochem) and 30 μM of the peptide substrate Crosstide for 10 min at 30°C. The reaction was terminated by centrifugation and the supernatants spotted on P81 phosphocellulose paper. After washing 4 times with 0.5% phosphoric acid and once with 95% ethanol, radioactivity was

determined by scintillation counting. PKCζ was immunoprecipitated with 2 μg PKCζ/λ antibody at 4°C followed by the addition of Protein A/G agarose (30 μl) for an additional 2 h. The immunocomplexes were washed twice with lysis buffer and twice with kinase assay buffer (50 mM Tris, pH 7.5, 5 mM $MgCl_2$, 0.1 mM Na_3VO_4, 0.1 mM $Na_4P_2O_7$, 0.1 mM NaF and 0.1 mM PMSF) and activity assayed as described by Standaert (19).

Measurement of Akt dephosphorylation:
Akt pSer473 dephosphorylation was determined in living adipocytes in situ and in cell lysates in vitro. Following the 18 h incubation, adipocytes were washed and re-stimulated with 100 nM insulin for 15 min at 37°C followed by the addition of 100 μM 2-DG and 5 μM rotenone to deplete cellular ATP as previously described (30,32). The cells were then incubated at either 37°C or 30°C for various times, rapidly washed, and lysed in buffer containing 250 mM sucrose. Cell lysates were subjected to SDS-PAGE and immunoblotted for total and pSer473 Akt as above. To determine dephosphorylation activity *in vitro*, lysates were prepared from adipocytes incubated for 18 h with or without HG/HI. Phosphorylated Akt immunoprecipitated from insulin-stimulated control adipocyte lysates was used as substrate. The immunocomplexes were washed twice with lysis buffer and twice with phosphatase assay buffer (100 mM HEPES, pH 7.5, 150 mM NaCl, 2 mM EDTA, 1 mM EGTA, and 1 mM DTT) and used immediately. Akt dephosphorylation was inititated by adding equal amounts of immunoprecipitated phosphorylated Akt protein to 50 μg cell lysates from control and resistant adipocytes and incubated in phosphatase buffer at 30°C for the times indicated. The reaction was stopped by the addition of Leammli sample buffer and boiling for 5 min. The extent of Akt pSer473 was assessed by immunoblotting as above.

Transfection of adipocytes:
Freshly isolated adipocytes were transiently transfected by electroporation as described previously (31,33). Briefly, 0.4 ml of adipocyte suspension (lipocrit of 60%) was added to 0.4-cm gap-width cuvettes with equal volumes of DMEM containing 7.5 μg of plasmid encoding various proteins and electroporated in the Gene Pulser Xcell TM Electroporation System (CE Module, Bio-Rad) by two pulses of 25 μF at 800 V followed by one pulse of 1,050 μF at 200V. Transfected cells were washed and incubated with DMEM containing 5% BSA for at least 18 h.

GLUT4 translocation determined by fluorescence microscopy.
Primary adipocytes were electroprated as described above with pQB125 plasmid encoding hemagglutinin-GLUT4-green fluorescent protein (HA-GLUT4-GFP) (S.W.Cushman, NIH, Bethesda, MD). After induction of insulin resistance, washing and restimulation with insulin as described above, cells were incubated with anti-GFP and mouse monoclonal anti-hemagglutinin antibody (1:150) and donkey anti-mouse IgG antibody conjugated with rhodamine red (1:100), fixed in 4% paraformaldehyde in PBS, and mounted on glass slides using Vectashield mounting medium as described (31). Fluorescence was observed using the Leica TCS SP2 Confocal Laser Scanning Microscope and analyzed with Leica Confocal Software. The intensities of the red fluorescence (cell surface GLUT4) were corrected for the green (total GLUT4) in all experiments and extent of translocation relative to control determined.

In vivo studies:
Female Wistar rats (Charles River, Quebec) were cannulated as described with the carotid artery for sampling and jugular vein for infusion (34). Rats were allowed at least 3 days of recovery before infusions. All protocols and procedures were approved by the University of Toronto Animal Care Committee. Rats (n=8) were randomized and infused for 48h with either saline

NaCl (154 mmol/L) (n=4) or a variable infusion of 37.5% (wt/vol) glucose (n=4) to achieve and maintain plasma glucose at 20-22 mmol/L. This 48h hyperglycemic clamp has been previously demonstrated to result in hyperinsulinemia and insulin resistance (34, 35). After 48h infusion, rats were killed and perirenal adipose tissue obtained. Adipocytes were isolated as described above and stimulated with and without 10^{-7}M insulin for 30 min. Cell lysis, homogenization and immunoblotting were performed as described above.

Data Analysis:
Results are expressed as mean ± SE. Differences were compared by ANOVA followed by the Bonferroni multiple comparisons test. Values of $p<0.05$ were accepted as significant. Paired t-tests were performed for values of glucose uptake at different insulin concentrations (Fig.1A) and dephosphorylation assays at different time points (Fig.3). For insulin-stimulated glucose uptake, the concentrations of insulin required for half maximal stimulation, EC_{50}, were determined from dose-response curves using nonlinear regression sigmoidal (four-parameter logistic) curve fitting, and signifcant differences were determined using the F test (Graph PadPrism Version 4.0, Graph Pad Software, San Diego, CA).

Results

High glucose/insulin impairs glucose uptake and GLUT4 translocation:
When the responses of rat adipocytes to acute insulin stimulation were examined after incubation for 18 h in the presence of high glucose/insulin (20 mM glucose/100 nM insulin), the cells showed a consistent and marked decrease in 2-DG uptake at all concentrations of insulin (Fig.1A). At the maximum insulin concentration tested, glucose uptake was significantly lower in resistant cells (control 816±156 pmol/6x10^5 cells/3 min, resistant 326±27, $p<0.05$). Adipocytes treated with high glucose/insulin also showed a marked decrease in basal glucose uptake (control 240±71 pmol/6x10^5 cells/3 min, resistant 55±11, $p<0.001$) (Fig.1A).

Insulin stimulated glucose uptake in fat cells is mediated by GLUT4 which translocates from intracellular LDM (low density microsomes) to PM in response to insulin (10). In control cells under basal conditions, virtually all of the GLUT4 (96.4 ± 1%) was found in the LDM. Upon insulin stimulation the GLUT4 content in the LDM fraction was reduced to 25.9 ±6% while the PM GLUT4 content increased from 3.6 ± 1% to 74.1 ± 6%. Resistant cells showed a marked defect in GLUT4 translocation as the decrease in LDM GLUT4 and increase in PM GLUT4 after insulin stimulation were both lower (94.6 ± 2% in LDM basal; 5.3 ±2% in PM basal; 64.3 ± 6% in LDM insulin-stimulated, 35.7 ± 6% in PM insulin-stimulated, $p<0.05$ compared to control) (Fig.1B). In addition to GLUT4, rat adipocytes also contain GLUT1, a ubiquitously expressed glucose transporter thought to be responsible for basal glucose uptake (10). GLUT1 was found exclusively in the PM fraction and there was no significant increase upon insulin stimulation in either control or resistant cells (Fig.1C). In adipocytes treated with high glucose/insulin there was a marked decrease in GLUT1 content to 20 ± 10% of control ($p<0.05$), which likely accounts for the decrease in basal glucose uptake observed (Fig.1C).

High glucose/insulin impairs IRS-1 Tyr phosphorylation and downstream signalling:
To determine the site of the defect in the insulin signalling of GLUT4 translocation in the resistant cells, we examined insulin-stimulated Tyr phosphorylation of IRS-1, a substrate of the insulin receptor. High glucose/insulin treatment decreased IRS-1 Tyr phosphorylation in response to insulin compared to control cells (control basal 28 ± 6 %, control insulin, designated as 100%, resistant basal 27 ± 5 %, resistant insulin 57 ± 9 %; $p<0.05$, insulin-stimulated control

vs resistant; n=3) (Fig.2A). Although in some studies hyperinsulinemia has been reported to decrease total levels of IRS-1 by enhancing its degradation (36), under these conditions in primary adipocytes, we found no significant change in total IRS-1.

Activation of PI 3-kinase and Akt is necessary for GLUT4 translocation and glucose uptake (2,12,16). Consistent with the decrease in IRS-1 Tyr phosphorylation, high glucose/insulin treatment significantly decreased insulin-stimulated Akt Ser473 phosphorylation to 28.7 ± 5.1 % of control, ($p<0.05$) and Thr308 phosphorylation to 33.7 ± 8.2 % of control ($p<0.05$) (Fig.2B). Total levels of Akt were unchanged by high glucose/insulin treatment.

Phosphorylation of Akt at Ser473 and Thr308 correlates with enzyme activity. Indeed, insulin-stimulated activation of Akt was impaired by ~50% in high glucose/insulin treated cells compared to control cells (14.3 ± 2.8-fold over basal in control adipocytes and 7.8 ± 0.95-fold in resistant cells, $p<0.05$). Basal values did not differ (control designated as 1.0, resistant 0.91 ± 0.22) (Fig.2C). To confirm that endogenous *in vivo* Akt activity was decreased, we determined phosphorylation of GSK-3α/β. Insulin increased phosphorylation of GSK-3α/β in control adipocytes 4-fold which was decreased by ~30% in the resistant cells (control basal 24.9±9.9%, control insulin designated as 100%, resistant basal 23.2±11%, resistant insulin 70.4±6.7%, $p<0.05$ compared with control insulin). There was no change in total GSK-3α/β (Fig. 2B).

In adipose tissue insulin stimulates the Ser phosphorylation and activation of both Akt1/PKBα and Akt2/PKBβ isoforms (16, 17). However, experiments in knockout mice (37) and cultured cells (38) indicate that Akt2/PKBβ is primarily, if not entirely, responsible for signalling to glucose transport. Immunoprecipitation of Akt2/PKBβ from cell lysates with isoform-specific antibodies and immunoblotting with anti-pSer473 Akt (recognizes pSer474 Akt2/PKBβ) revealed that the high glucose/insulin induced defect applied to Akt2/PKBβ (Fig.2D).

It has been suggested that different defects in this model may depend more on the high glucose versus insulin (9). To determine which was predominant for Akt, adipocytes were incubated for 18 h in control medium, high glucose (20 mM) without insulin, high insulin (10^{-7}M) in the absence of glucose in medium supplemented with 1 mM pyruvate, or with combined HG/HI. While insulin alone induced the defect in Akt phosphorylation similar to that observed with combined glucose plus insulin, high glucose alone had no effect (Fig. 2E).

High glucose/insulin does not enhance Akt dephosphorylation:

Decreased AktSer473 phosphorylation could be due to impaired phosphorylation by an upstream kinase or increased dephosphorylation due to increased phosphatase activity. The latter has been previously reported in response to palmitate-induced insulin resistance (39). Thus, the rate of Akt pSer473 dephosphorylation was examined. *In vitro,* dephosphorylation was assayed by incubating immunoprecipitated pSer473 Akt from insulin-stimulated control adipocytes together with cell lysates from either control or high glucose/insulin treated adipocytes. Akt pSer473 was dephosphorylated at similar rates (Fig.3A). Since phosphatase activity may have been lost or altered by cell disruption, Akt dephosphorylation was measured *in situ* in intact cells. Cellular ATP was depleted by 90 – 95% within 5 min of addition of rotenone and 2-DG (not shown) thereby inhibiting kinase activity. At 37°C Akt dephosphorylation was rapid, with 70% of pSer473 dephosphorylated within 2 min and there was no difference in the rate of dephosphorylation in resistant adipocytes compared to control (Fig.3B). At 30°C the overall rate of pSer473 dephosphorylation was slower and at 2 min, Akt Ser473 phosphorylation remained significantly higher in high glucose/insulin (HG/HI) treated cells suggesting a slightly decreased

phosphatase activity in insulin resistant cells (Fig.3C). However, this trend was not significant taking into account the entire time course. These findings indicate that the decreased phosphorylation of Akt Ser473 in response to insulin in the insulin resistant adipocytes was not due to accelerated dephosphorylation.

High glucose/insulin treatment is associated with chronic activation of PCK-ζ:

High glucose has been shown to activate various isoforms of PKC in multiple tissues (40, 41), most commonly PKC-β and δ. The latter are stimulated by DAG (diacylglycerol), which is increased in response to elevated glucose. In cultured fibroblasts, PKC activation by exposure to high glucose has been implicated in the induction of insulin resistance (42). To test for PKC isoform activation in adipocytes, the cells were homogenized and separated into membrane and cytosolic fractions and translocation from cytosol to membrane, considered evidence of activation, was determined. While there were no significant changes in PKC-$\beta_{1/2}$, PKC-δ, or PKC-ε membrane protein content, a significant translocation of PKC-ζ, an atypical PKC, was observed in resistant compared to control cells ($p<0.01$) (Fig.4A). Activation of PKC-ζ, a Ser/Thr kinase, is associated with phosphorylation of its kinase loop by PDK-1 (18, 43). Since phosphorylation of the PDK-1 site on Akt, namely Thr308, was decreased in the HG/HI treated cells (Fig. 2B), we determined whether PKC-ζ activation by insulin was impaired. In control cells, insulin increased PKC-ζ activity by 184± 31.4% compared to basal ($p<0.05$) (Fig. 4B). In contrast, in HG/HI treated cells PKC-ζ was already activated in the basal state despite the removal of the HG/HI medium by the washing procedure. Thus, basal PKC-ζ activity in the resistant cells was elevated to a similar extent as the insulin-stimulated controls (238±28.7% of control basal, $p<0.005$) and there was no significant increase in activity upon restimulation with insulin (resistant insulin 254± 54.2% of control basal) (Fig. 4B).

The defect in Akt Ser473 phosphorylation is reversed by inhibition of PKC-ζ:

Although PKC-ζ has been shown to have a positive role in the insulin stimulation of glucose transport, it has also been reported to inhibit insulin action at the level of IRS-1 (23, 24, 26). In addition, in non-insulin target cells, PKC-ζ has been reported to interact with and inhibit Akt (27, 29). To investigate whether PKC-ζ could have a role in downregulating Akt activation in this model of insulin resistance, adipocytes were cotransfected with expression vectors encoding wild-type (WT) myc-Akt (Akt 1)and DN PKC-ζ (rat PKC-ζ 2-592 K281R, J.W. Soh, Columbia University, NY) (44). It has been previously demonstrated that upon electroporation, the same population of cells takes up both vectors and expresses the proteins (33). We first confirmed that expressed WT myc-Akt manifested the identical defect in insulin-stimulated Ser473 (Fig.5A) and Thr308 (not shown) phosphorylation in the high glucose/insulin model. Cotransfection of DN PKC-ζ in control cells resulted in a small (≤ 10%), but consistent, decrease in Ser473 phosphorylation. However, in resistant cells, the defect in insulin-stimulated Ser473 phosphorylation of myc-Akt was reversed (control + pcDNA3 designated as 100%, control + DN-PKC-ζ 92.2%, resistant + pcDNA 64.7%, resistant + DN PKC-ζ 89.2%) (Fig. 5A). It should be noted that the transfected myc-tagged Akt is visible slightly above the endogenous Akt in the immunoblots. Considering a transfection efficiency of between 30 – 50%, (documented in preliminary experiments with a GFP expressing vector and with HA-GLUT4-GFP, and by immunoblotting of total PKC-ζ), we noted that in experiments in which DN PKC-ζ reversed the defect, there was an ~4.5-fold overexpression compared to endogenous PKC-ζ (n=4), while in those without reversal, expression of DN-PKC-ζ was < 1.5-fold (n=4) indicating the requirement

of an increased ratio of DN-mutant to WT to achieve suppression of PKCζ activity. A second caveat of these experiments was that if PKC-ζ inhibition by the DN mutant occurred early, the reversal could have been due, at least in part, to an inhibition of glucose uptake. This was not likely since the Akt defect could be induced by high insulin even in the absence of glucose (Fig. 2E).

In contrast to transfection with DN-PKC-ζ, overexpression of constitutively active membrane-targeted, myristoylated CA-PKC-ζ (provided by Alex Toker, 18) resulted in inhibition of insulin-stimulated Ser473 phosphorylation of the coexpressed myc-Akt, similar to the defect caused by high glucose/insulin, and enhanced the high glucose/insulin effect (Fig. 5B). Previous observations that overexpression of PKC-ζ could increase glucose uptake independent of insulin (19-22) raised the possibility that this effect on Akt phosphorylation could be indirect; that is, mediated entirely by enhanced glucose uptake in the transfected population of cells, or that PKC-ζ was not sufficient by itself to induce the defect. To eliminate the potential effect of glucose uptake, adipocytes were cotransfected as above and incubated in glucose and insulin free medium supplemented with 1 mM pyruvate. CA-PKC-ζ inhibited insulin-stimulation of Ser473 phosphorylation of coexpressed myc-Akt determined in anti-myc immunoprecipitates (Fig. 5C).

To examine endogenous proteins and other signaling components, we applied a cell permeable myristoylated PKC-ζ specific pseudosubstrate inhibitor (PS). High glucose/insulin treatment markedly impaired insulin-stimulated IRS-1 Tyr phosphorylation and association of the p85 subunit of PI3-kinase, Akt Ser473 and Thr308 and GSK3α/β phosphorylation (Fig.6A). Since inhibition of PKC-ζ has been reported to block insulin-stimulated glucose uptake, and indeed, we confirmed that a 30 min preincubation with the PS inhibitor blocked both insulin-stimulated glucose uptake and PKC-ζ activation (not shown), it was not desirable to add the PS inhibitor from the start of the incubation prior to the induction of the insulin resistance. However, insulin resistance in this model is well established after 8 h of incubation (9 and data not shown). Addition of the PKC-ζ PS inhibitor for only the final 2 h (16-18 h) reversed the impairment of IRS-1 Tyr phosphorylation and the association of the p85. PS treatment also markedly improved impaired Akt Ser473 and Thr308 phosphorylation observed in resistant cells and normalized insulin-stimulated GSK3 phosphorylation (Fig. 6A). To demonstrate specificity of the PKC-ζ PS inhibitor, in separate experiments the resistant cells were treated for the final 2 h with 10 μmol/L of a cell permeable PKC-α/β specific pseudosubstrate inhibitor (N-myristoylated PKC-α/β amino acid residues 20-28, Calbiochem-Millipore). There was no rescue of the AktSer473 phosphorylation defect with the PKC-α/β PS inhibitor (Fig. 6B). It should be noted that high insulin and high glucose are not required to maintain the insulin resistance during this 2 h incubation as washing the cells and reincubating in control medium for the 2 h did not reverse insulin resistance (Suppl. Fig. 1).

Inhibition of PKC-ζ restores insulin sensitivity of glucose uptake:

To test whether the Akt defect contributed to the decrease in glucose transport, the resistant adipocytes were exposed to the PKC-ζ PS inhibitor for the final 2 h as described above. It was first determined that treatment of control adipocytes for 2 h with the PKC-ζ inhibitor, followed by the washing procedure allowed for full recovery of glucose uptake (not shown). Reversal of the Akt phosphorylation defect with the PKC-ζ PS inhibitor was associated with a restoration of relative GLUT4 translocation from LDM to PM seen at maximum insulin concentrations (Fig. 7A). Similarly, assessment of GLUT4 translocation with HA-tagged GLUT4-GFP using

confocal microscopy revealed that the defect induced by exposure to high glucose/insulin was reversed by the PKC-ζ PS inhibitor (Fig. 7B).

Assessment of 2DG uptake revealed that insulin sensitivity was normalized by the PKC-ζ PS inhibitor (Fig. 7C and Suppl Fig 2A). The concentration of insulin required to stimulate 2-DG uptake by 50%, EC50, was increased in resistant cells (control 8.8 pmol/L, 95% confidence interval (CI) 5.2-14.5; resistant 27.0 pmol/L, 95% CI 15-49, $p<0.0001$). After treatment with the PKC-ζ PS inhibitor the EC50 in control adipocytes was 4.8 pmol/L, CI 2.9-8.1, and in resistant cells was restored to control (9.3 pmol/L, CI 6.2-13.8) (Fig. 7C). Similar to the results with Akt Ser473 phosphorylation, the PKC α/β specific PS inhibitor did not alter the defect in glucose uptake induced by HG/HI (Suppl. Fig. 2B). It should be noted that downregulation of insulin receptors (IRs) by high concentrations of insulin has been reported in a number of cell types and could have contributed to decreased insulin sensitivity (1-3). However, we observed only a minor and inconsistent decrease (0 – 15%) in cell surface IRs under these conditions and no change in total cellular IRs or Tyr phosphorylation of the IR β-subunit as would be expected with downregulation (Suppl Fig. 3A). The maximum response to insulin was also decreased in resistant cells and significantly improved in the presence of the PKC-ζ inhibitor (Fig. 7D). While the difference between maximum insulin-stimulated glucose uptake in resistant cells treated with PSI and control cells did not reach statistical significance ($p=0.08$), we noted that it remained consistently lower. It has been shown that even with a significant reduction in Akt activation in the order of 75-80%, a high concentration of insulin is able to stimulate maximum glucose transport (45). These data suggest that an additional defect is present that accounts for the decrease in maximum insulin response. Consistent with this interpretation, we observed that total GLUT4 content was significantly decreased under these conditions (Suppl. Fig. 3B).

IRS-1 Ser318 phosphorylation is involved in insulin resistance:

It has been demonstrated that insulin resistance may be caused by Ser phosphorylation of IRS-1 (11,25). Phosphorylation of IRS-1 Ser318 has been demonstrated to be mediated by PKC-ζ and associated with negative regulation of insulin signaling in BHK and cultured muscle cells (26, 46). We examined this possibility by cotransfecting cells with CA-PKC-ζ and either wild-type or mutant IRS-1 S318A, previously described (46). We first confirmed that IRS-1 Ser318 was phosphorylated in response to insulin and blocked by the PKC-ζ PS inhibitor (Suppl. Fig. 4A). Overexpression of CA-PKC-ζ decreased insulin-stimulated Tyr phosphorylation of IRS-1 and Akt Ser473 phosphorylation in WT-Akt and WT–IRS-1 cotransfected cells (Fig. 5B and Fig. 8A). These effects were partially prevented in cells cotransfected with IRS-1 S318A (Fig. 8A). Importantly, the defect in IRS-1 Tyr phosphorylation and Akt Ser473 and Thr308 phosphorylation induced by HG/HI was also diminished in adipocytes cotransfected with IRS-1 S318A (Fig. 8B). We noted that similar results for IRS-1 Tyr phosphorylation were obtained in these transfection experiments in immunoblots of total cell lysates or IRS-1 immunoprecipitates. The high degree of correction of the defect in Tyr phosphorylation with IRS-1 S318A to 69 ± 6.3% of control with CA-PKC-ζ and 88 ± 4.3% with HG/HI may be accounted for by the high efficiency of transfection combined with overexpression so that transfected IRS-1 (WT or mutant) was in the order of 70 – 80% of total immunoprecipitated IRS-1. These results indicate that the HG/HI induced model of insulin resistance in rat adipocytes is due, in part, to phosphorylation of Ser318 of IRS-1 mediated by enhanced activation of PKC-ζ.

Akt Thr34 phosphorylation by PKC-ζ is involved in insulin resistance:

PKC-ζ has been reported to physically interact with Akt leading to phosphorylation of the Akt-PH domain on Thr34 and preventing activation of the enzyme by insulin (27, 29). We confirmed that Akt Thr34 phosphorylation was enhanced by chronic incubation in the high glucose/insulin medium and blocked by the PKC-ζ PS inhibitor (Suppl. Fig. 4B). Cotransfection of rat adipocytes with CA-PKC-ζ and WT myc-Akt or HA-Akt T34A (described in 29) showed that the CA-PKC-ζ-induced decrease in insulin-stimulated Akt Ser473 and Thr308 phosphorylation was significantly less with the mutant Akt T34A (Fig. 8C). Transfection of adipocytes with HA-Akt T34A also partially restored the diminished insulin-stimulated Akt Ser473/Thr308 phosphorylation induced by HG/HI (Fig. 8D). Significantly, the HG/HI-induced defect in Ser473/Thr308 phosphorylation was completely recovered by cotransfection of adipocytes with both IRS-1 S318A and Akt T34A (Fig. 8E).

In vivo hyperglycemia-induced insulin resistance is associated with increased IRS-1 Ser318 and Akt Thr34 phosphorylation:

We previously demonstrated that 48h infusion of glucose to maintain concentrations of 20-22 mM induces hyperinsulinemia and insulin resistance (34,35). Thus, rat adipocytes were isolated at the end of 48h infusion of saline or glucose and cells stimulated or not with insulin. Immunoblotting revealed insulin resistance in adipocytes from glucose-infused rats with defects in Akt Ser473 and IRS-1 Tyr phosphorylation (Fig. 9A,B). This was associated with an augmented phosphorylation of Akt Thr34 and IRS-1 Ser318 in the resistant cells (Fig. 9). In contrast, IRS-1 Ser307 phosphorylation was not increased (Fig.9B). This was consistent with our observations in the in vitro studies which did not show any increase in phosphorylation of IRS-1 Ser307 or IRS-1 Ser636/639 in the insulin resistant state (Suppl Fig. 5). Furthermore, the high glucose infusion resulted in enhanced phosphorylation of PKC-ζ Thr410, the PDK-1 site and a marker of its activation (Fig. 9C). These in vivo data support the cultured adipocyte studies and indicate that PKC-ζ mediates HG/HI-induced insulin resistance via phosphorylation of IRS-1 Ser318 and Akt Thr34.

Discussion

Both hyperglycemia and hyperinsulinemia have been demonstrated to cause insulin resistance in all three metabolic target tissues, fat, muscle and liver (2,3, 47). In adipocytes this has been most clearly demonstrated in primary culture of rat adipocytes exposed to increasing concentrations of glucose in combination with insulin (9, 47). In this model, a decrease in insulin sensitivity, i.e. a rightward shift in the dose-response curve of glucose uptake and a decrease in maximum response to insulin, as well as a decrease in basal glucose uptake were all observed. The defect in insulin-stimulated glucose uptake was associated with a defect in the movement of GLUT4 from an internal membrane compartment, LDM, to the PM (Fig.1). On the other hand, the decrease in basal glucose uptake was associated with a marked decrease in PM GLUT1 content. In the context of this change in basal glucose uptake and GLUT1, the assessment of insulin resistance may be underestimated by the commonly used expression of the increase in glucose uptake as fold of basal. Since the extent of insulin stimulation is accounted for by translocation and potential activation of GLUT4, the absolute change in glucose uptake caused by insulin is, in this case, a more accurate reflection of insulin action.

The signaling of GLUT4 translocation and glucose uptake by insulin, although not completely understood, requires Tyr phosphorylation of IRS-1 by the insulin receptor and the subsequent binding and activation of PI3-kinase. Lipid phosphorylation results in activation of

Akt and PKC-ζ, both implicated in mediating GLUT4 translocation. In this study, insulin-stimulated IRS-1 Tyr phosphorylation, IRS-1 association with p85 and activation of Akt were significantly decreased in adipocytes chronically exposed to HG/HI. In a similar model, others have reported that decreased insulin sensitivity in adipocytes exposed to HG/HI was associated with a decrease in total IRS-1 protein (48). In contrast, we did not find a significant change in IRS-1 protein content in the resistant adipocytes. Similarly, HG/HI induced insulin resistance preceded IRS-1 protein depletion in human adipocytes (49). In one study in which primary adipocytes were cultured in 10% FCS and the duration of exposure was longer, 24 h, high glucose alone induced insulin resistance (48). However, we (Fig. 2E) and others (47) did not observe this in 0.5% FBS, suggesting that serum factors are required.

The mechanism of Akt activation entails its recruitment to the PM and phosphorylation on two sites, Thr308 and Ser473 by two separate enzymes, PDK-1 and the mTOR/rictor complex, respectively (3, 12-14). In this study the high glucose/insulin-induced impaired Akt activation was associated with a marked decrease in both Thr308 and Ser473 phosphorylation. The reduction of Akt phosphorylation could have been due to decreased kinase activity or an increase in dephosphorylation. Elevated phosphatase activity of a PP2A family enzyme has been implicated in the Akt defect induced by the FFA, palmitate (39). In contrast, in this HG/HI model, we found no change in the rate of Akt pSer473 dephosphorylation. The cause and significance of the minimally decreased Akt dephosphorylation in the insulin resistant adipocytes at 30°C is not clear.

As phosphorylation of Akt Thr308 by PDK-1 in the resistant cells was impaired, we assayed another downstream target of PDK-1, namely PKC-ζ. Unexpectedly, we found that PKC-ζ activity was elevated in the basal state in the resistant cells and not further stimulated by insulin. This persistent activation, in spite of extensive washing to remove the HG/HI, was unique in that all other parameters examined, including IRS-1 Tyr phosphorylation, association of p85 subunit of PI3-kinase, Akt Thr308 and Ser473 phosphorylation and glucose transport, returned to basal levels under similar conditions. The absence of persistent basal Akt Thr308 phosphorylation in the resistant cells suggests that PDK-1 may not be responsible for the elevated PKC-ζ activity. PDK-1-independent activation of PKC isoforms, including PKC-ζ, has been reported, but the mechanism is not well understood (50). It is also possible that PDK-1 retains some activity and that lack of membrane translocation of Akt prevents its Thr308 phosphorylation. This could be explained by the observed Akt Thr34 phosphorylation (29).

Elevated PKC-ζ activity has also been observed in skeletal muscle in the *in vivo* pathophysiological setting of high fat diet-induced insulin resistance (51). PKC-ζ has been reported to negatively regulate insulin action in hepatocytes (23) and adipocytes (24) by promoting Ser phosphorylation of IRS-1, associated with decreased insulin-stimulated IRS-1 Tyr phosphorylation and activation of PI 3-kinase. Furthermore, exposure of pancreatic β-cells to elevated FFAs resulted in chronic activation of PKC-ζ which was associated with impaired IGF-1 activation of Akt (52). Together, these findings suggest that PKC-ζ may function as a negative feedback regulator. To probe the role of PKC-ζ in the HG/HI-induced insulin resistant adipocytes, we used genetic and pharmacological approaches. Cotransfection of DN PKC-ζ with WT-Akt was able to abrogate the induction of the impairment in Akt Ser473 phosphorylation in the presence of HG/HI. However, two caveats of this experiment were considered. First, a high degree of PKC-ζ overexpression was required for the dominant negative action. Second, impairment of glucose uptake by PKC-ζ inhibition could have contributed. Thus, we utilized a cell permeable PKC-ζ PS inhibitor peptide. Incubation with the PKC-ζ inhibitor during the

final 2 h of the HG/HI treatment reversed the Akt defect while simple removal of the HG/HI medium for 2 h, or addition of a PKC-α/β PS inhibitor, did not. While other PKC isoforms have been implicated in mediating insulin resistance (reviewed in 2) the lack of effect of the PKCα/β inhibitor combined with minimal, nonsignificant membrane increases of these other isoforms suggest that in the HG/HI model PKC-ζ is the major mediator. The observed increase in vivo in PKC-ζ phosphorylation of its PDK-1 activation-loop site supports this conclusion.

To prove the requirement and sufficiency of chronic PKC-ζ activation to induce this defect, the adipocytes were cotransfected with expression vectors for CA-PKC-ζ and myc-WT-Akt and incubated in medium without glucose and insulin to avoid enhanced glucose uptake in the transfected cells. CA-PKC-ζ was able to recapitulate the defect in Akt Ser473 phosphorylation. These results indicate that the elevated PKC-ζ activity is responsible for the defect in Akt phosphorylation induced by HG/HI.

IRS-1 Ser/Thr phosphorylation is a major mechanism leading to insulin resistance and several specific phosphorylation sites and kinases have been identified (reviewed in 2). One of these sites, Ser318 of IRS-1, has been demonstrated to be a target of PKC-ζ, and its phosphorylation was stimulated in BHK cells by 60 min of insulin treatment and associated with decreased IRS-1 Tyr phosphorylation and reduced complex formation between IR and IRS-1(26). In the present study, the defects in IRS-1 Tyr phosphorylation induced by either CA-PKC-ζ transfection or by HG/HI treatment were corrected in cells transfected with IRS-1 S318A. Of interest, a study in skeletal muscle cells found that, in contrast to prolonged stimulation, acute insulin stimulation of IRS-1 Ser318 phosphorylation was not inhibitory, but rather enhanced insulin signal transduction (46). This potential sequentially different function of one phosphorylation site suggests the possibility that other Ser/Thr sites and/or other kinases may be required in addition to IRS-1 Ser318 to mediate the insulin resistance. A previous study in C2C12 cultured muscle cells reported that IRS-1 Ser318 phosphorylation was associated with activation of JNK and the PI3K/mTOR pathway (53). JNK, mTOR and the p70S6K Ser/Thr kinases have been documented to cause insulin resistance associated with IRS-1 phosphorylation (3). While we have documented a short term (30-60 min) stimulation of JNK and phosphorylation of IRS-1 Ser307, a major target site of JNK, by insulin in adipocytes (31), this was not detected at 18 h in vitro (Suppl. Fig. 5) or in vivo (Fig. 9B). Furthermore, IRS-1 Ser636, a target of phosphorylation by the mTOR pathway was not elevated (Suppl. Fig. 5). One other kinase implicated in insulin resistance and downstream of PKC-ζ is IKKβ (2, 54). However, the major target site of IKKβ is also Ser307, which was not phosphorylated under these conditions in vitro or in vivo. In addition, in our previous study we did not detect insulin-stimulated IKKβ activation in these primary adipocyte cultures (31). Together these data indicate that these kinases, i.e. JNK, TOR/p70S6K, IKKβ, are not responsible for the maintenance of insulin resistance in this longer term HG/HI model. It should be noted that PKC-ζ has been suggested to target other IRS-1 Ser sites, i.e. Ser612, Ser498 and Ser570 (numbering of rat IRS-1, 53), of which Ser570 appeared to be key to the induction of insulin resistance (55). Furthermore, a number of other Ser sites, e.g. Ser408, are phosphorylated in response to insulin which may be targeted by PKC-ζ (23, 25). Whether PKC-ζ IRS-1 phosphorylation sites other than Ser 318 contribute to the insulin resistance in this model requires further investigation.

Although the transfection of adipocytes with IRS-1 S318A restored IRS-1 Tyr phosphorylation by insulin, Akt phosphorylation in these transfected cells was only partly recovered. It has been reported that PKC-ζ directly interacts with and represses the activity of

Akt (27, 29) and dissociates from Akt upon growth factor and insulin stimulation, thereby allowing Akt to become activated. Recent studies showed that in L6 cells, ceramide-activated PKC-ζ physically interacts with Akt and phosphorylates the Akt–PH domain on Thr34, leading to the inhibition of Akt binding to PI-3,4,5P_3 and inhibition of kinase activation by insulin (29). In this study, we observed that adipocytes incubated with HG/HI, Akt Thr34 phosphorylation was significantly increased in vitro (Suppl. Fig. 4) and in vivo (Fig. 9). Transfection of adipocytes with mutant Akt T34A partially restored the impaired Akt Ser473 and Thr308 phosphorylation induced by either cotransfected CA-PKC-ζ or HG/HI treatment. Thus, PKC-ζ causes insulin resistance in this model by at least two mechanisms, targeting IRS-1 as well as Akt directly. Indeed, cotransfection of WT Akt with a combination of both mutants, IRS-1 S318A and Akt T34A, completely prevented the defect in Akt phosphorylation induced by HG/HI incubation. This is the first study documenting that chronic HG/HI-induced insulin resistance, a metabolic model of early type 2 diabetes, in a physiological target tissue is mediated by simultaneous dual targeting of signaling proteins by PKC-ζ.

At the same time, we noted that a defect in maximum insulin response of glucose transport was sustained even in the face of complete restoration of signaling to Akt (Fig.7D) and the normalization of the shift in the insulin dose-response curve. This appears to be due to a decrease in total cellular GLUT4 content (Suppl. Fig. 3B) so that fewer absolute numbers of transporters are recruited despite a normal relative translocation. This decrease in GLUT4 content was induced by insulin and enhanced by high glucose (Suppl. Fig. 3B). The mechanism of this second defect remains to be elucidated.

In summary, this study demonstrates for the first time that PKC-ζ plays a key role as a mediator of chronic insulin resistance in a metabolic pathophysiologic state in adipocytes in vitro and in vivo. Furthermore, in this hyperinsulinemia/hyperglycemia model, we demonstrate the simultaneous dual targeting of IRS-1 and Akt.

This chronic negative feedback loop has been challenging to address in the context of glucose uptake due to the fact that PKC-ζ also participates positively in insulin-stimulated glucose uptake. These data indicate that PKC-ζ should be included in the group of Ser/Thr kinases that mediate insulin resistance induced by various metabolic and inflammatory or stress states (Fig. 10) (56). The mechanism by which PKC-ζ remains chronically activated under these conditions requires further investigation. Identifying the protein(s) responsible could lead to new therapeutic strategies that, while blocking negative feedback, preserve the positive role of PKC-ζ in insulin action.

Acknowledgements

This work was supported by a grant from the Canadian Institutes for Heath Research (CIHR, Grant No. 38009). EB and CC were supported in part by studentships from the Banting and Best Diabetes Centre, University of Toronto. LL was supported by a visiting Scholarship from the China Scholarship Council, China.

This work was supported by: A grant from the Canadian Institutes for Heath Research (CIHR, Grant No. 38009). EB and CC were supported in part by studentships from the Banting and Best Diabetes Centre, University of Toronto. LL was supported by a visiting Scholarship from the China Scholarship Council, China.

Canadian Institutes for Health Research (CA), 38009, I George Fantus; Banting and Best Diabetes Centre, University of Toronto http://dx.doi.org/10.13039/501100000064,

Studentships for EB and CC, I George Fantus; China Scholarship Council http://dx.doi.org/10.13039/501100004543, Visiting Scholarship for LL, I George Fantus

Corresponding Author and to Whom Correspondence should be addressed: I. George Fantus, M.D., Departments of Medicine & Physiology, Mount Sinai Hospital, Joseph and Wolfe Lebovic Building, 60 Murray Street, 5th Floor, Rm 5028, Toronto, Ontario M5T 3L9, Canada, Telephone: 416-586-8665, Fax: 416-361-2657, E-mail: gfantus@mtsinai.on.ca

Disclosure Statement: The authors have nothing to disclose.

References

1. DeFronzo RA, Ferrannini E. Insulin resistance. A multifaceted syndrome responsible for NIDDM, obesity, hypertension, dyslipidemia, and atherosclerotic cardiovascular disease. Diabetes Care. 1991;14:173-194.
2. Taniguchi CM, Emanuelli B, Kahn CR. Critical nodes in signalling pathways: insights into insulin action. Nat Rev Mol Cell Biol. 2006;**7**:85-96.
3. Schenk S, Saberi M, Olefsky JM. Insulin sensitivity: modulation by nutrients and inflammation. J Clin Invest. 2008;118:2992-2002.
4. Boden G. Role of fatty acids in the pathogenesis of insulin resistance and NIDDM. Diabetes 1997;46:3-10.
5. Tremblay F, Lavigne C, Jacques H, Marette A 2007 Role of dietary proteins and amino acids in the pathogenesis of insulin resistance. Annu Rev Nutr 27:293-310.
6. Blondel O, Bailbe D, Portha B. Insulin resistance in rats with non-insulin dependent diabetes induced by neonatal (5 days) streptozotocin: evidence for reversal following phlorizin treatment. Metabolism. 1990;39:787-793.
7. Rossetti L, Smith D, Shulman GI, Papachristou D, DeFronzo RA. Correction of hyperglycemia with phlorizin normalizes tissue sensitivity to insulin in diabetic rats. Clin Invest. 1987;79:1510-1515.
8. Hager SR, Jochen AL, Kalkhoff RK. Insulin resistance in normal rats infused with glucose for 72 h. Am J Physiol. 1991;260:E353-E362.
9. Garvey WT, Olefsky JM, Matthaei S, Marshall S. Glucose and insulin co-regulate the glucose transport system in primary cultured adipocytes. A new mechanism of insulin resistance. J Biol Chem. 1987;262:189-197.
10. Mueckler M. Family of glucose-transporter genes. Implications for glucose homeostasis and **diabetes**. Diabetes 1990;39:6-11.
11. White MF. Family of glucose-transporter genes. Implications for glucose homeostasis and **diabetes**.Recent Prog Horm Res. 1998;53:119-138.
12. Rameh LE, Cantley LC. The role of phosphoinositide 3-kinase lipid products in cell function. J Biol Chem. 1999;274:8347-8350.
13. Alessi DR, Andjelkovic M, Caudwell B, Cron P, Morrice N, Cohen P, Hemmings BA. Mechanism of activation of protein kinase B by insulin and IGF-1. EMBO J. 1996;15:6541-51.
14. Sarbassoy DD, Guertin DA, Ali SM, Sabatini DM. Phosphorylation and regulation of Akt/PKB by the rictor-mTOR complex. Science. 2005;307:1098-1101.
15. Kohn AD, Summers SA, Birnbaum MJ, Roth RA. Expression of a constitutively active Akt Ser/Thr kinase in 3T3-L1 adipocytes stimulates glucose uptake and glucose transporter 4 translocation. J Biol Chem. 1996;272:31372-31378.

16. Whiteman LE, Cho H, Birnbaum MJ. Role of Akt/protein kinase B in metabolism. Trends Endocrinol Metab. 2002;13:444-451.
17. Scheid MP, Woodgett JR. PKB/AKT: functional insights from genetic models. Nat Rev Mol Cell Biol. 2001;2:760-768.
18. Chou MM, Hou W, Johnson J, Graham LK, Lee MH, Chen CS, Newton AC, Schaffhausen BS, Toker A. Regulation of protein kinase C zeta by PI 3-kinase and PDK-1. Curr Biol. 1998;8:1069-1077.
19. Standaert ML, Bandyopadhyay G, Perez L, Price D, Galloway L, Poklepovic A., Sajan MP, Cenni V, Sirri A, Moscat J, Toker A, Farese RV. Insulin activates protein kinases C-zeta and C-lambda by an autophosphorylation-dependent mechanism and stimulates their translocation to GLUT4 vesicles and other membrane fractions in rat adipocytes. J Biol Chem. 1999;274:25308-25316.
20. Kotani K, Ogawa W, Matsumoto M, Kitamura T, Sakaue H, Hino Y, Miyake K, Sano W, Akimoto K, Ohno S, Kasuga M. Insulin activates protein kinases C-zeta and C-lambda by an autophosphorylation-dependent mechanism and stimulates their translocation to GLUT4 vesicles and other membrane fractions in rat adipocytes. Mol Cell Biol. 1998;18:6971-6982.
21. Liu L-Z, Zhao H-L, Zuo J, Ho SKS, Chan JCN, Meng Y, Fang F-D, Tong PCY. Protein kinase Czeta mediates insulin-induced glucose transport through actin remodeling in L6 muscle cells. Mol Biol Cell. 2006;17:2322-2330.
22. Hodgkinson CP, Mander A, Sale GJ. Protein kinase-zeta interacts with munc18c: role in GLUT4 trafficking. Diabetologia. 2005;48:1627-1636.
23. Liu YF, Paz K, Herschkovitz A, Alt A, Tennenbaum T, Sampson SR, Ohba M, Kuroki T, LeRoith D, Zick Y. Insulin stimulates PKC zeta-mediated phosphorylation of insulin receptor substrate-1 (IRS-1). A self-attenuated mechanism to negatively regulate the function of IRS proteins. J Biol Chem. 2001;276:14459-14465.
24. Ravichandran LV, Esposito DL, Chen J, Quon MJ. Protein kinase C-zeta phosphorylates insulin receptor substrate-1 and impairs its ability to activate phosphatidylinositol 3-kinase in response to insulin. J Biol Chem. 2001;276:3543-3549.
25. Liu J-F, Herschkovitz A, Boura-Halfon S, Ronen D, Paz K, LeRoith D, Zick Y. Serine phosphorylation proximal to its phosphotyrosine binding domain inhibits insulin receptor substrate 1 function and promotes insulin resistance. Mol. Cell. Biol. 2004;24: 9668-9681.
26. Moeschel K, Beck A, Weigert C, Lammers R, Kalbacher H, Voelter W, Schleicher ED, Häring H-U, Lehmann R. Protein kinse C-zeta-induced phosphorylation of Ser318 in insulin receptor substrate-1 (IRS-1) attenuates the interaction with the insulin receptor and the tyrosine phosphorylation of IRS-1. J Biol Chem. 2004;**279**:25157-25163.
27. Doornbos RP, Theelen M, van der Hoeven PC, van Blitterswijk WJ, Verkleij AJ, van Bergen en Henegouwen PM. Protein kinase Czeta is a negative regulator of protein kinase B activity. J Biol Chem. 1999;274:8589-8596.
28. Farese RV, Sajan MP, Yang H, Li P, Mastorides S, Gower WR Jr, Nimal S, Choi CSKim S, Shulman GI, Kahn CR, Braun U, Leitges M. Muscle-specific knockout of PKC-lambda impairs glucose transport and induces metabolic and diabetic syndromes. J Clin Invest. 2007;117:2289-2301.
29. Powell DJ, Hajduch E, Kular G, Hundal HS. Ceramide disables 3-phosphoinositide binding to the pleckstrin homology domain of protein kinase B (PKB)/Akt by a PKCzeta-dependent mechanism. Mol Cell Biol. 2003;23:7794-7808.

30. Tang S, Le-Tien H, Goldstein BJ, Shin P, Lai R, Fantus IG. Decreased in situ insulin receptor dephosphorylation in hyperglycemia-induced insulin resistance in rat adipocytes. Diabetes. 2001;50:83-90.
31. Beard KM, Lu H, Ho K, Fantus IG. Bradykinin augments insulin-stimulated glucose transport in rat adipocytes via endothelial nitric oxide synthase-mediated inhibition of Jun NH2-terminal kinase. Diabetes. 2006;55:2678-2687.
32. Dlugosz JA, Munk S, Kapor-Drezgic J, Goldberg HJ, Fantus IG, Scholey JW, Whiteside CI. Stretch-induced mesangial cell ERK1/ERK2 activation is enhanced in high glucose by decreased dephosphorylation. Am J Physiol Renal Physiol. 2000;279:F688-F697.
33. Quon MJ, Zarnowski MJ, Guerre-Millo M, de la Luz Sierra M, Taylor SI, Cushman SW. Transfection of DNA into isolated rat adipose cells by electroporation: evaluation of promoter activity in transfected adipose cells which are highly responsive to insulin after one day in culture. Biochem Biophys Res Commun. 1993;194:338-346.
34. Tang C, Han P, Oprescu AI, Lee SC, Gyulkhandanyan AV, Chan GNY, Wheeler MB, Giacca A. Evidence for a role of superoxide generation in glucose-induced β-cell dysfunction in vivo. Diabetes 56: 2722-2731, 2007.
35. Tang C, Koulajian K, Schuiki I, Zhang L, Desai T, Ivovic A, Wang P, Robson-Doucette C, Wheeler MB, Minassian B, Volchuk A, Giacca A. Glucose-induced beta cell dysfunction in vivo in rats: link between oxidative stress and endoplasmic reticulum stress. Diabetologia 55: 1366 1379, 2012.
36. Rui L, Yuan M, Frantz D, Shoelson S, White MF. WSOCS-1 and SOCS-3 block insulin signaling by ubiquitin-mediated degradation of IRS1 and IRS2. J Biol Chem. 2002;277:42394-42398.
37. Cho H, Mu J, Kim JK, Thorvaldsen JL, Chu Q, Crenshaw EB, Kaestner KH, Bartolomei MS, Shulman GI, Birnbaum MJ. Insulin resistance and a diabetes mellitus-lilke syndrome in mice lacking the protein kinase Akt2 (PKB beta). Science 2001;292: 1728-1731.
38. Jiang ZY, Zhou QL, Coleman KA, Chouinard M, Boese Q, Czech MP. Insulin signaling through Akt/protein kinase B analyzed by small interfering RNA-mediated gene silencing. Proc Natl Acad Sci USA. 2003;100: 7569-7574.
39. Cazzolli R, Carpenter L, Biden TJ, Schmitz-Peiffer C. A role for protein phosphatase 2A-like activity, but not atypical protein kinase C zeta, in the inhibition of protein kinase B/Akt and glycogen synthesis by palmitate. Diabetes. 2001;50:2210-2218.
40. Lee TS, Saltsman KA, Ohashi H, King GL. Activation of protein kinase C by elevation of glucose concentration: poroposal for a mechanism in the development of diabetic vascular complications. Proc Natl Acad Sci USA. 1989;86: 5141-5.
41. Xia P, Inoguchi T, Kern TS, Engerman RL, Oates PJ, King GL. Characterization of the mechanism for the chronic activation of diacylglycerol-protein kinase C pathway in diabetes and hypergalactosemia. Diabetes. 1994;43:1122-1129.
42. Berti L, Mosthaf L, Kroder G, Kellerer M, Tippmer S, Mushack J, Seffer E, Seedorf K, Haring H. Glucose-induced translocation of protein kinase C isoforms in rat-1 fibroblasts is paralleled by inhibition of the insulin receptor tyrosine kinase. J Biol Chem. 1994;269:3381-3386.
43. LeGood JA, Ziegler WH, Parakh DB, Alessi DR, Cohen P, Parker PJ. Protein kinase C isotypes controlled by phosphoinositide 3-kinase through the protein kinase PDK1. Science. 1998;281:2042-2045.

44. Soh J-W, Lee E-H, Pyrwes R, Weinstein IB. Novel roles of specific isoforms of protein kinase C in activation of the c-fos serum response element. Mol Cell Biol. 1999;19: 1313-1324.
45. Wang Q, Somwar R, Bilan PJ, Liu Z, Jin, J, Woodgett JR, Klip A. Protein kinase B/Akt participates in GLUT4 translocation by insulin in L6 myoblasts. Mol Cell Biol. 1999; 19:4008-4018.
46. Weigert C, Hennige AM, Brischmann T, Beck A, Moeschel K, Schauble M, Brodbeck K, Haring H-U, Schleicher ED, Lehmann R. The phosphorylation of Ser318 of insulin receptor substrate 1 is not per se inhibitory in skeletal muscle cells but is necessary to trigger the attenuation of the insulin-stimulated signal. J. Biol Chem. 2005;280: 37393-37399.
47. Marshall S, Garvey WT, Traxinger RR. New insights into the metabolic regulation of insulin action and insulin resistance: role of glucose and amino acids. FASEB J. 1991;5:3031-3036.
48. Buren J, Liu HX, Lauritz J, Eriksson JW. High glucose and insulin in combination cause insulin receptor substrate-1 and -2 depletion and protein kinase B desensitization in primary cultured rat adipocytes: possible implications for insulin resistance in type 2 diabetes. Euro J Endocrinol. 2003;148: 157-167.
49. Renstrom F, Buren J, Svensson M, Eriksson JW. Insulin resistance induced by high glucose and high insulin precedes insulin receptor substrate 1 protein depletion in human adipocytes. Metabolism. 2007;56:190-198.
50. Grunicke HH, Spitaler M, Mwanjewe J, Schwaiger W, Jenny M, Ueberall F. Regulation of cell survival by atypical protein kinase C isozymes. Adv Enzyme Regul. 2003;43:213-228.
51. Tremblay F, Lavigne C, Jacques H, Marette A. Defective insulin-induced GLUT4 translocation in skeletal muscle of high fat-fed rats is associated with alterations in both Akt/protein kinase B and atypical protein kinase C (zeta/mabda) activities. Diabetes. 2001;**50**:1901-1910.
52. Cousin SP, Hügl SR, Wrede CE, Kajio H, Myers MG Jr, Rhodes CJ. Free fatty acid-induced inhibition of glucose and insulin-like growth factor 1-induced deoxyribonucleic acid synthesis in the pancreatic beta-cell line INS-1. Endocrinol. 2001;142: 229-240.
53. Mussig K, Fiedler H, Staiger H, Weigert C, Lehmann R, Schleicher ED, Haring H-U. Insulin-induced stimulation of JNK and the PI3-kinase/mTOR pathway leads to phosphorylation of serine 318 of IRS-1 in C2C12 myotubes. Biochem Biophys Res Comm. 2005;335:819-825.
54. Lallena M-J, Diaz-Meco MT, Bren G, Paya CV, Moscat J. Activation of IkappaB kinase beta by protein kinase C isoforms. Mol Cell Biol. 1999;19: 2180-2188.
55. Sommerfeld ML, Metzger S, Stosik M, Tennagels N, Eckel J. In vitro phosphorylation of insulin receptor substrate 1 by protein kinase C-zeta: functional analysis and identification of novel phosphorylation sites. Biochemistry. 2004;**43**: 5888- 5901.
56. Farese RV, Sajan MP. Metabolic functions of atypical protein kinase C: "good" and "bad" as defined by nutritional status. Am J Physiol. 2010;298: 385-394.

Fig. 1. Effect of high glucose/insulin on glucose uptake and glucose transporters (GLUTs). Adipocytes were incubated at 37°C for 18 h in either DMEM containing 5.6 mM glucose (Control, open circles) or containing 20 mM glucose and 100 nM insulin (Resistant, closed circles). Cells were then extensively washed as described and incubated with the indicated concentrations of insulin for 30 min, followed by (A) assay of 2-deoxyglucose (2DG) uptake. Data shown are mean ± SE of 3 independent experiments (*$p < 0.001$, Resistant vs Control). (B) LDM and PM fractions were prepared from control and resistant cells and 30 μg protein resolved by SDS-PAGE and immunoblotted with anti-GLUT4 or (C) anti-GLUT1 antibody.

Immunoblots shown are from one of 3 independent experiments with similar results (see text for means ± SE).

Fig. 2. Effect of high glucose/insulin on IRS-1 tyrosine phosphorylation and downstream signalling. Adipocytes were incubated for 18 h as described in Fig.1. in Control (5.6 mM glucose) and Resistant (20 mM glucose and 100 nM insulin) (HG/HI)conditions, washed and restimulated in the presence and absence of 100 nM insulin. IRS-1 was immunoprecipitated from cell lysates (500 μg), resolved by SDS-PAGE and immunoblotted with (A) anti-IRS-1 and anti-pY antibodies (B). Forty μg protein were resolved by SDS-PAGE and immunoblotted with anti-Akt, anti-phospho-Akt (pSer473 and pThr308), anti-GSK-3 3α/β (GSK-3) and anti-pSer9/pSer21 GSK-3 α/β (pGSK-3) antibodies. (C) Total Akt was immunoprecipitated from cell lysates and *in vitro* kinase activity was determined using the peptide substrate Crosstide. Data shown are mean ± SE of 3 independent experiments (* $p< 0.05$, Resistant vs Control). (D) Akt2 was immunoprecipitated and immunoblotted with anti-Akt2 and anti-pSer473 Akt. Insulin-stimulated Akt2 Ser474 phosphorylation was reduced by 56±6.8% in insulin resistant cells (n=3, $p<0.01$) (E) Cells were incubated for 18 h in the presence of 5.6 mM glucose (control), 20 mM glucose without insulin (HG), 100 nM insulin without glucose supplemented with pryruvate (HI) or combined (HG/HI) as above. Cell lysates were prepared and immunoblotted with anti-total and anti-pSer473 Akt. The decrease in insulin-stimulated Akt phosphorylation was significant for HG/HI (64±9.4%) and HI (51±5.0%) ($p<0.05$ for both compared with control) (n=3) while there was no difference with HG (107±6.8% of control, n=3).

Fig. 3. Effect of high glucose/insulin on Akt dephosphorylation. Adipocytes were incubated for 18 h as described in Fig. 2, washed and restimulated in the presence and absence of insulin. (A) Cell lysates (50 μg protein) from control (open circles) and resistant (closed circles) adipocytes were incubated with equal amounts of phosphorylated Akt immunoprecipitated from insulin-stimulated control adipocytes. *In vitro* dephosphorylation was allowed to proceed as described at 30°C and at the times indicated aliquots removed, boiled in SDS sample buffer, resolved by SDS-PAGE and immunoblotted with anti-pSer473Akt and anti-total Akt antibodies. After correction for total Akt the relative intensities of pSer473 were plotted as % of maximum insulin-stimulated Akt phosphorylation prior to dephosphorylation. (B and C) After restimulation of control (open circles) and resistant (closed circles) adipocytes with 100 nM insulin for 15 min, 100 μM 2-DG and 5 μM rotenone were added to deplete cellular ATP and the incubation continued at 37°C (B) or 30°C (C) as described. At the indicated times, cells were lysed and pSer473 Akt and total Akt immunoblotted and relative pSer473 Akt dephosphorylation determined as above. *$p<0.05$, Control versus resistant.

Fig. 4. Effect of high glucose/insulin on PKC translocation. Adipocytes were incubated for 18 h as described in Fig. 2. Cell lysates and cell membranes were prepared as described. (A) Equal aliquots of protein of total cell lysates and cell membrane fractions were resolved by SDS-PAGE and immunoblotted with antibodies against the various PKC isoforms indicated. Representative immunoblots are shown. Graphs depict means ± SE (n=3) of membrane-associated PKC isoforms in Control and Resistant (HG/HI) adipocytes. **$p<0.01$, R versus C PKC-ζ. Total cell lysate PKC protein content was not significantly different for any isoform. (B) PKC-ζ was immunoprecipitated from cell lysates and *in vitro* kinase activity determined as

described. Data shown are mean ± SE of 6 independent experiments. *p < 0.05 Control basal vs Control insulin, *** p < 0.005, Resistant basal vs Control basal.

Fig. 5 Effect of dominant-negative (DN) and constitutively active (CA) PKC-ζ on Akt phosphorylation. Adipocytes were transiently transfected with wild-type myc-epitope tagged Akt (WT-Akt) along with (A) dominant-negative, PKC-ζ K281R (DN PKC-ζ) or (B) CA-PKC-ζ by electroporation. Cells transfected with empty vector (pcDNA3) served as control. After equilibration in DMEM for 1 h, the cells were washed and incubated for 18 h as described in Fig. 2. After washing, the adipocytes were restimulated in the presence and absence of 100 nM insulin for 15 min, cell lysates were prepared and equal aliquots of protein separated by SDS-PAGE and immunoblotted with anti-pSer473 and anti-PKCζ/λ antibodies. The transfected myc-Akt is differentiated from endogenous Akt by its slower migration. (A) Overexpression of DN PKC-ζ prevented the high glucose/insulin-induced decrease in Akt Ser473 phosphorylation by 90% (n=2) (see text for details). (B) Insulin-stimulated Akt pSer473 was decreased compared with control (100%) by high glucose/insulin to 49± 11.2% (p<0.05), by CA-PKC-ζ to 45± 10.5% (p<0.05) and by combined HG/HI and CA-PKC-ζ to 24±8.7% (P<0.01) (n=3). (C) Transfected cells were incubated in a medium without glucose supplemented with pyruvate, cell lysates were prepared and immunoblotting performed as above. CA-PKC-ζ decreased insulin-stimulated Akt pSer473 to 42±1.0% (p<0.01, n=3).

Fig. 6 Inhibition of PKC-ζ reverses the high glucose/insulin induced defect in IRS-1 Tyr phosphorylation and downstream signaling. Adipocytes were incubated for 18 h as described in Fig. 2 with or without addition of (A) 10 μM myristoylated PKC-ζ specific PS inhibitor (PKC-ζ PS) or (B) 10 μM PKC-α/β PS inhibitor for the final 2 h (16-18 h). Cells were then washed and restimulated for 15 min in the presence and absence of 100 nM insulin. Cell lysates were immunoprecipitated with anti-IRS-1 antibodies and immunoblotted with anti-pY, anti-IRS-1 and anti-p85 as indicated. Total cell lysates were immunoblotted with anti-pSer473, anti-pThr308, anti-Akt, anti-phospho-GSK3 and anti-GSK3 as indicated. Immunoblots are representative of 3 separate experiments and the intensities of the phosphorylated proteins were corrected for total protein in each experiment determined by reprobing of stripped membranes. In the absence of PKC-ζ inhibitor the high glucose/high insulin (HG/HI) treatment decreased insulin-stimulated IRS-1 pY to 44.5±9.6% of control (p<0.01), IRS-1 association of p85 to 46.9±0.4% of control (p<0.01), Akt pSer473 to 17.7±5. 4% and Akt pThr308 to 24.7±0.6% of control (p<0.005 for both) and pGSK3 to 49.1±2.7% of control (p<0.005) (n=3). Two h of treatment with PKC-ζ inhibitor blocked these effects of HG/HI. IRS-1 pY 94.0±7.8%, p85 association 101.8±9.1%, Akt pSer473 92.5±4.4%, Akt pThr308 84.1±9.4% and pGSK3 100.5±10.7% (p=NS compared with control for all except Akt pThr 308 which was not completely reversed (p<0.05), n=3). In contrast, in the presence of the PKC-α/β inhibitor insulin-stimulated Akt pSer473 remained decreased by ~ 60% in resistant cells. Mean ± SE (n=3) insulin-stimulated Akt pSer473 corrected for total Akt (fold of control basal); Control 5.66 ± 1.68, Resistant 2.28 ± 0.71, Control + PKC α/β PS 5.44 ± 1.97, Resistant + PKC α/β PS 1.92 ± 0.49.

Fig. 7 Inhibition of PKC-ζ reverses the high glucose/insulin-induced defect in GLUT4 translocation and insulin insensitivity of glucose uptake. Adipocytes were incubated and

treated with PKC-ζ PS inhibitor as described in Fig. 6. (A) PM and LDM were prepared and immunoblotted with anti-GLUT4 antibody as described in Fig. 1. Immunoblots are representative of 3 separate experiments. The % (mean ±SE) of total GLUT4 in the PM after insulin stimulation were: control 66.0±7.6, HG/HI 40.4±5.3 ($p< 0.01$) and HG/HI+PKC-ζ PS 78.5±3.8 (p=NS versus C, $P<0.001$ versus R). The % (mean ± SE) decrease in LDM GLUT4 after insulin stimulation were: control 59.5±6.3, HG/HI 12.2 ± 4.2 ($p<0.01$) and HG/HI + PKC-ζ PS 70.0 ± 3.2% (p=NS versus C, $p< 0.001$ versus R) (n=3) (B) (Color online). Adipocytes were transfected with a HA-GLUT4-GFP expression vector by electroporation and cells treated as in Fig.6. Confocal microscopic images were obtained and analyzed as described. Images are representative of 4 – 7 separate experiments. In 2 experiments in which all 8 conditions were performed together and 35-50 cells analyzed per condition the mean relative translocation was: Control basal 1.0; Control + Insulin 2.85; Control + PS inhibitor basal 1.25; Control + PS inhibitor + Insulin 3.0; Resistant basal 1.01; Resistant + Insulin 1.36; Resistant + PS inhibitor basal 1.51; Resistant + PS inhibitor + Insulin 2.93. (C) Cells incubated in control medium (●,○), or high glucose/insulin containing medium (■,□) were treated with (broken lines, open symbols) or without (solid lines, filled symbols) PKC-ζ PS inhibitor for the final 2 h. Glucose uptake was performed as in Fig. 1. Results shown are values for glucose uptake normalized for basal uptake, designated as 0, and maximum uptake, designated as 100%, in each condition. Values are the mean ± SE of 4-7 experiments performed in duplicate. *$p<0.05$ Resistant vs all other conditions (see text for details). (D) Maximum insulin-stimulated glucose uptake from experiments in C. Values shown are mean ± SE insulin-stimulated glucose uptake (pmol/$5x10^6$ cells/3 min); C (Control) 439±27.2, R (resistant) 240 ±8.2, C + PKC-ζ PS 455±71.8, R + PKC-ζ PS 383±34.0. *$p<0.01$ R versus C and C+PSI and $p< 0.05$ R versus R + PSI (n=4).

Fig. 8 Transfection of IRS-1 S318A or Akt T34A reverses impaired IRS-1 Tyr and Akt Ser 473 phosphorylation induced by either cotransfected CA-PKC-ζ or by treatment with high glucose/insulin. (A) Adipocytes were cotransfected with IRS-1 S318A (318), CA-PKC-ζ, (CA) and WT-Akt as indicated and cell lysates prepared. Transfected WT myc-Akt was immunoprecipitated with anti-myc and immunoblotting performed as described. Immunoblots are representative of 3 separate experiments. The values (mean ± SE) for insulin-stimulated IRS-1 pY corrected for total IRS-1 and myc-Akt pSer473 corrected for total myc-Akt are shown in the graphs below. Insulin-stimulated control (C/I) values were designated as 100%. *$p<0.05$ versus all other groups.. (B) Adipocytes were cotransfected with IRS-1 S318A (318) and WT myc-Akt and incubated in high glucose/insulin, washed and restimulated with insulin. Cell lysates were prepared and immunoprecipitated with anti-myc antibodies and immunoblotted as described. Immunoblots are representative of 3 separate experiments. Values (mean ± SE) for insulin-stimulated IRS-1 pY and myc-Akt pSer473 and pThr308 are shown in the graphs below. ** $p<0.01$ and *$p<0.05$, versus all other groups. (C) Adipocytes were cotransfected with WT myc-Akt or mutant HA-Akt T34A and either pcDNA 3.0 (empty vector) or CA-PKCζ (CA) and cell lysates prepared, immunoprecipitated with anti-myc or anti-HA and immunoblotted as above. Immunoblots are representative of 3 separate experiments. Values (means ± SE) for insulin-stimulated myc-Akt pSer473 and pThr 308 and HA-Akt T34A pSer473 and pThr 308 are shown in the graphs below. **$p<0.01$ versus all other groups. (D) Adipocytes were transfected with WT myc-Akt or HA-Akt T34A and incubated in control or HG/HI medium as in Fig. 2. Immunoblots are representative of 3 separate experiments. Values (mean ± SE) for insulin-

stimulated myc-Akt pSer 473 and pThr 308 and HA-Akt T34A pSer 473 and pThr 308 are shown in the graphs below. **p<0.01 versus all other groups. (E) Adipocytes were transfected as indicated and incubated in control or HG/HI medium as in D. Cell lysates were prepared and immunoprecipitation and immunoblotting performed as above. Immunoblots are representative of 3 separate experiments. Values (mean ± SE) for insulin-stimulated myc-Akt pSer 473 and pThr 308 and HA-Akt T34A pSer 473 and pThr 308 are shown in the graphs below **p<0.01 versus all other groups.

Fig. 9 In vivo 48h hyperglycemia/hyperinsulinemia causes insulin resistance associated with augmented IRS-1 Ser318,Akt Thr34 and PKC-ζ pThr 410 phosphorylation. Rats were infused for 48h with glucose to maintain hyperglycemia 20-22 mM, (R=resistant) (n=4) or saline (C=control) (n=4). Adipocytes were isolated, washed and stimulated or not with 100 nM insulin (I) as described in Methods. Lysates were prepared, equal amounts of protein separated by SDS-PAGE and immunoblotted with A) antibodies to total Akt, Akt pSer473, Akt pThr34; B) total IRS-1, phosphotyrosine (pY), IRS-1 pSer318 and IRS-1 pSer307; and C) total PKC-ζ and PKC-ζ pThr410. Representative immunoblots are shown and the graphs below depict densitometric values (mean±SE) of phosphorylated proteins corrected for total Akt (A), total IRS-1 (B) total PKC-ζ (C) and expressed relative to control basal (C/B). A) Akt pSer 473, **p<0.01, C/I vs all other groups; Akt pThr34 *p<0.05, R vs C. B) pY, ** p<0.01 C/I vs all other groups; IRS-1 pSer318, ** p<0.01 R vs C. C) PKC-ζ pThr 410, *p<0.05 R vs C.

Fig. 10 (Color Online) PKC-ζ induces insulin resistance by dual targeting of IRS-1 and Akt. Insulin resistance is associated with a number of pathophysiological factors including elevated circulating levels of metabolites, AA (amino acids), glucose, FFA (free fatty acids); pro-inflammatory cytokines, e.g. TNF-α; oxidative stress ($O_2^{\cdot-}$) and chronic hyperinsulinemia. These in turn, activate various unique and interacting signaling pathways that commonly result in phosphorylation of IRS-1 to inhibit insulin action. Hyperinsulinemia combined with hyperglycemia activates several of these downstream pathways, e.g .JNK, which may exert rapid and short term negative feedback. PKC-ζ however, appears to remain chronically activated and sustains insulin resistance by phosphorylation of two targets, IRS-1 Ser 318 and Akt Thr 34. The role of PKC-ζ and phosphorylation of these targets in maintaining decreased insulin sensitivity in human subjects requires further study.

Antibodies used. RRID numbers are from **http://antibodyregistry.org**.

Antibody	Source	RRID
Akt	Cell Signaling Technology	AB_329827
Phospho-Akt (Ser473)	Cell Signaling Technology	AB_329825
Phospho-Akt (Thr308)	Cell Signaling Technology	AB_329828
AKT1 (phosphoT34)	Abcam	AB_2558095
Anti-Human Akt2 (F-7)	Santa Cruz Biotechnology	AB_626659
Phospho-PCKζ/λ (Thr410/403)	Cell Signaling Technology	AB_2168217
PKC zeta (C-20	Santa Cruz Biotechnology	AB_2300359
PCK beta (C-16	Santa Cruz Biotechnology	AB_2168968
PKC delta (C-17)	Santa Cruz Biotechnology	AB_632228
PKC epsilon (C-15)	Santa Cruz Biotechnology	AB_2237729
IRS-1	Cell Signaling Technology	AB_330333
Phospho Ser307-IRS-1	Millipore	AB_11213228
Anti-IRS1 Agarose Conjugated	Millipore	AB_310783
Phospho Ser318-IRS-1 (D51C3)	Cell Signaling Technology	AB_10695244
p-Tyr (PY99)	Santa Cruz Biotechnology	AB_628123

Glucose Transporter GLUT1	Novus	AB_790014
Glucose Transporter GLUT4	Millipore	AB_211989
Anti-P13 Kinase, p85 Polyclonal	Millipore	AB_310141
Anti-GSK-3 alpha/beta	Millipore	AB_11205766
Phospho-GSK-3 alpha/beta (S21/S9)	R and D Systems	AB_354880
c-Myc (9E10) antibody	Santa Cruz Biotechnology	AB_627268
HA.11 Monoclonal Antibody	Covance Research Products Inc	AB_10063630
Phospho Ser636/639 IRS-1	Millipore	AB_1587211

A

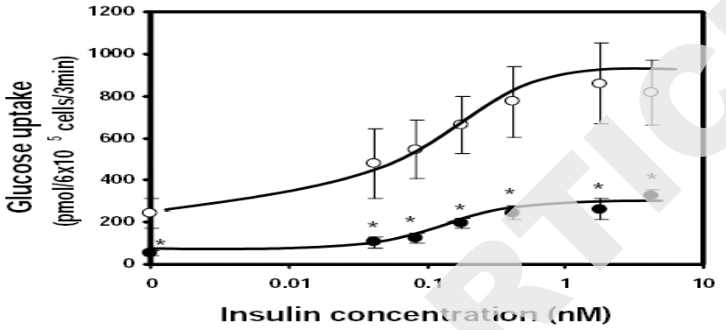

B

C

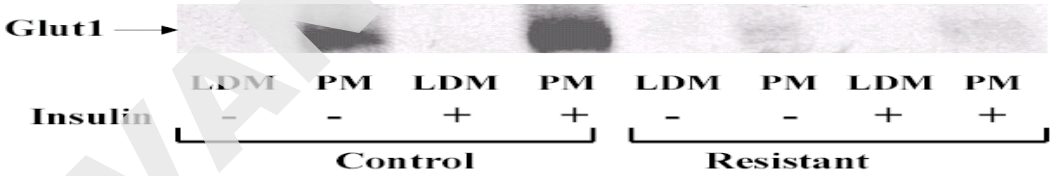

Fig. 1

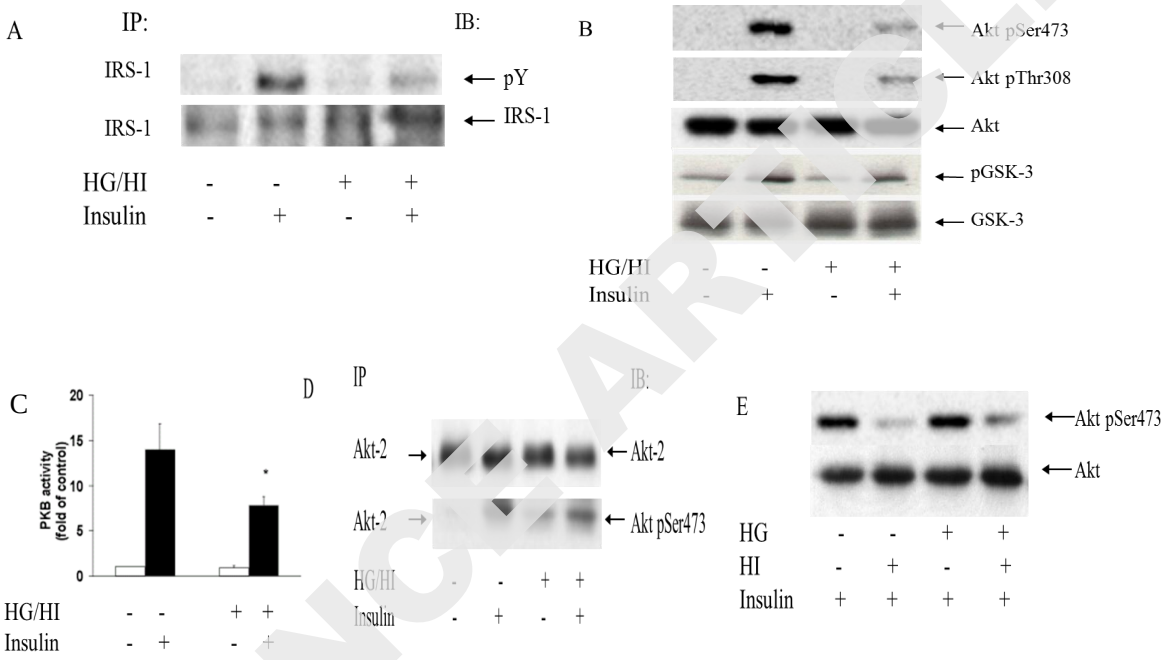

Fig. 2

A

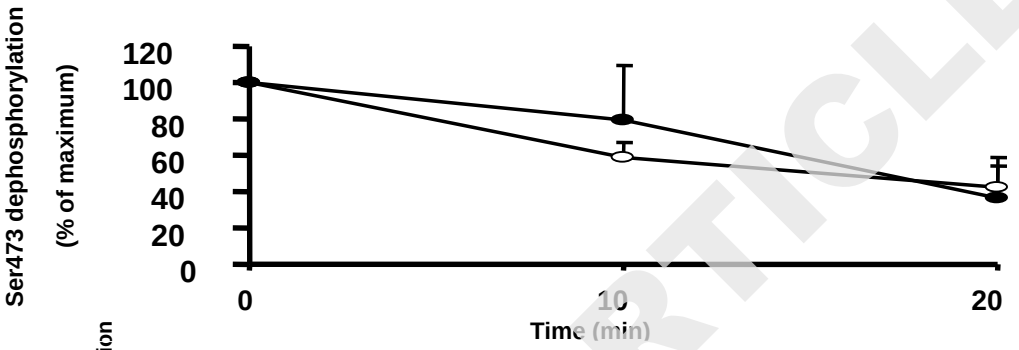

B

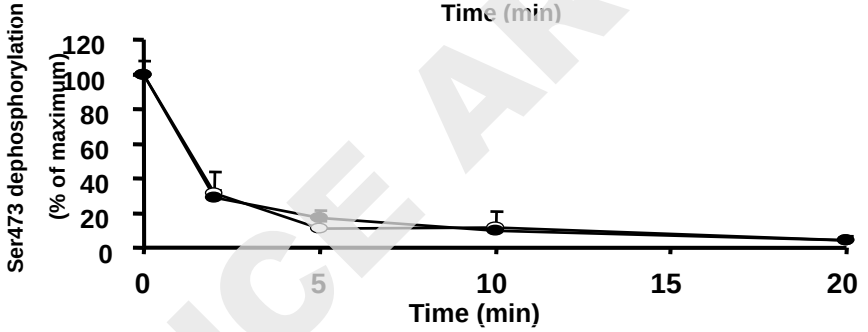

C

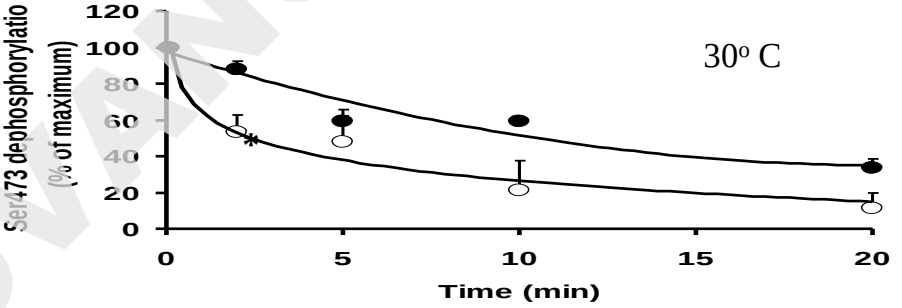

Fig. 3

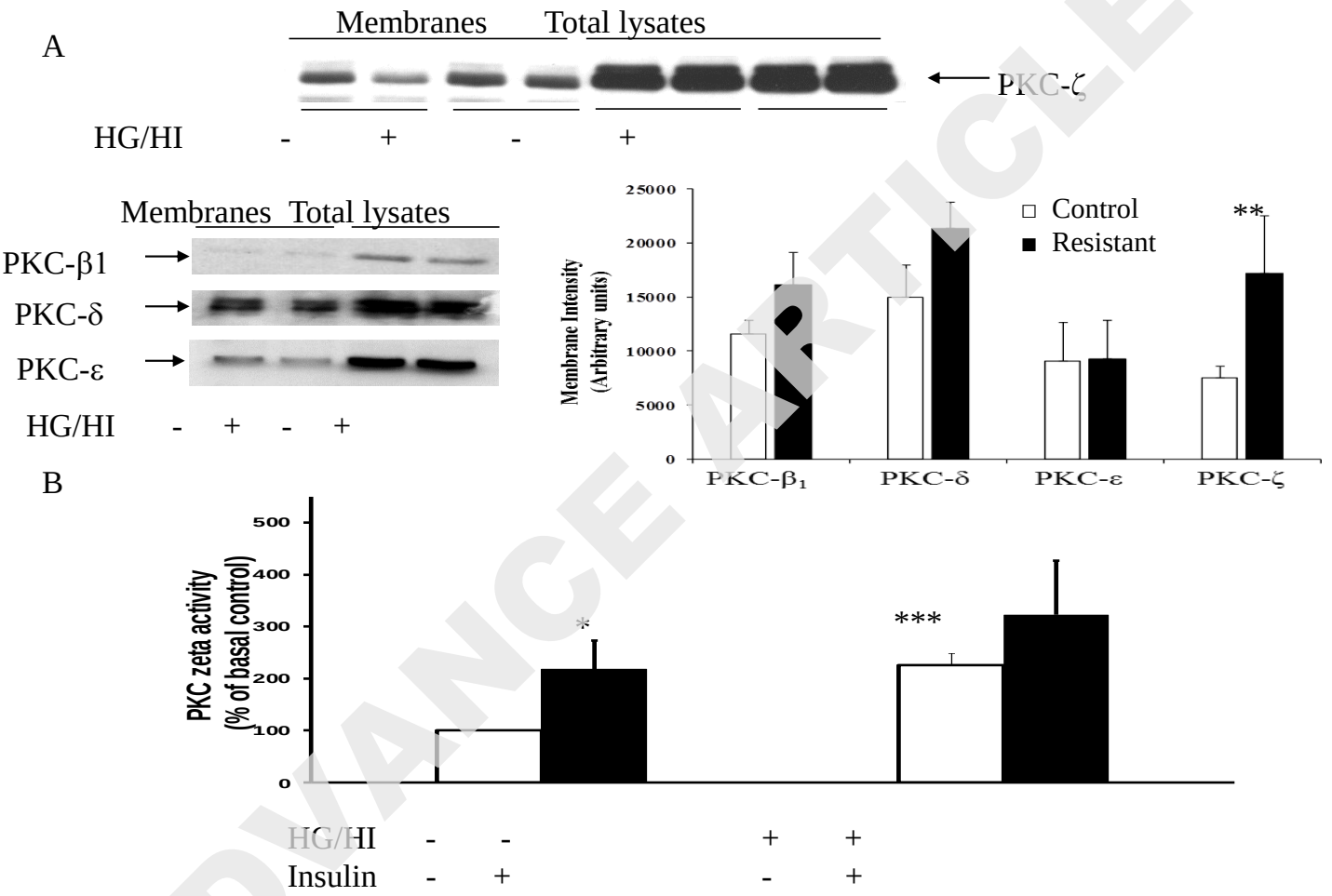

Fig. 4

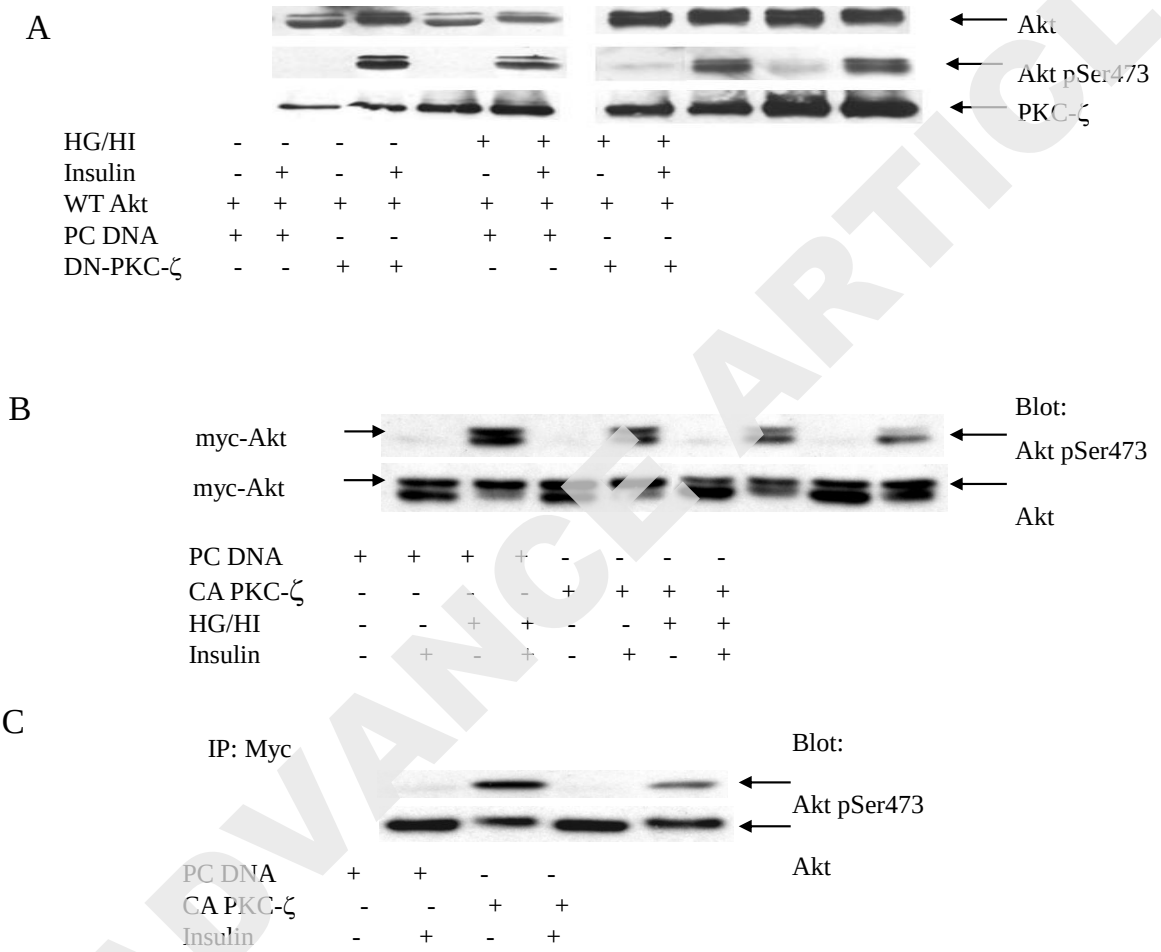

Fig. 5

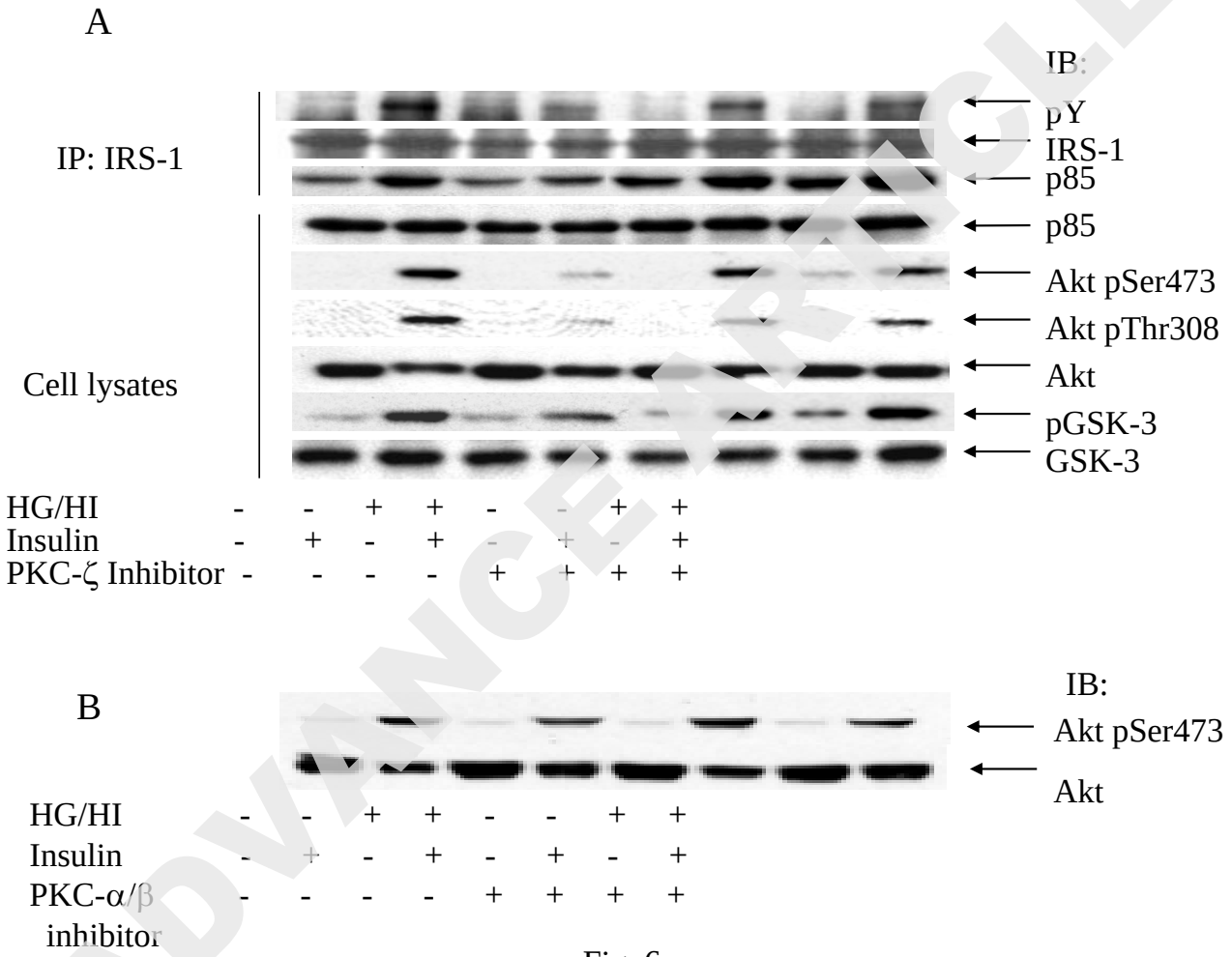

Fig. 6

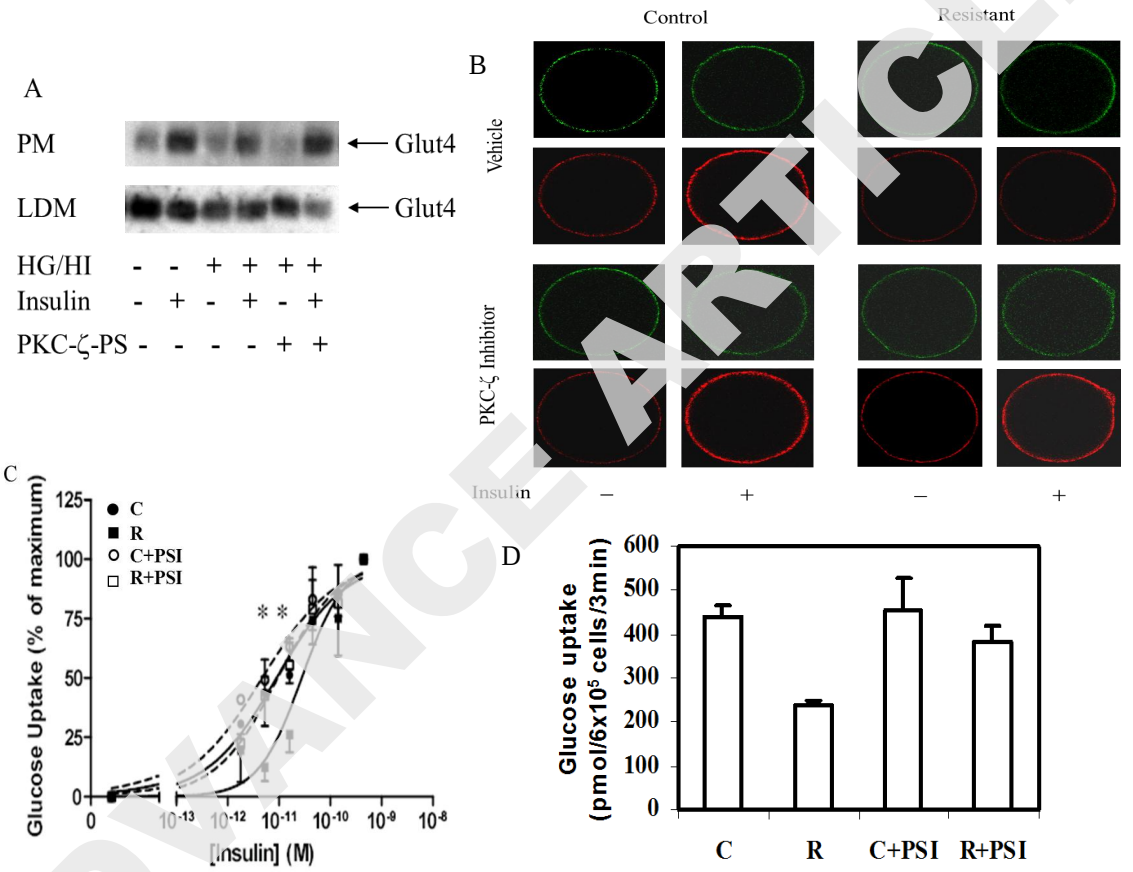

Fig. 7

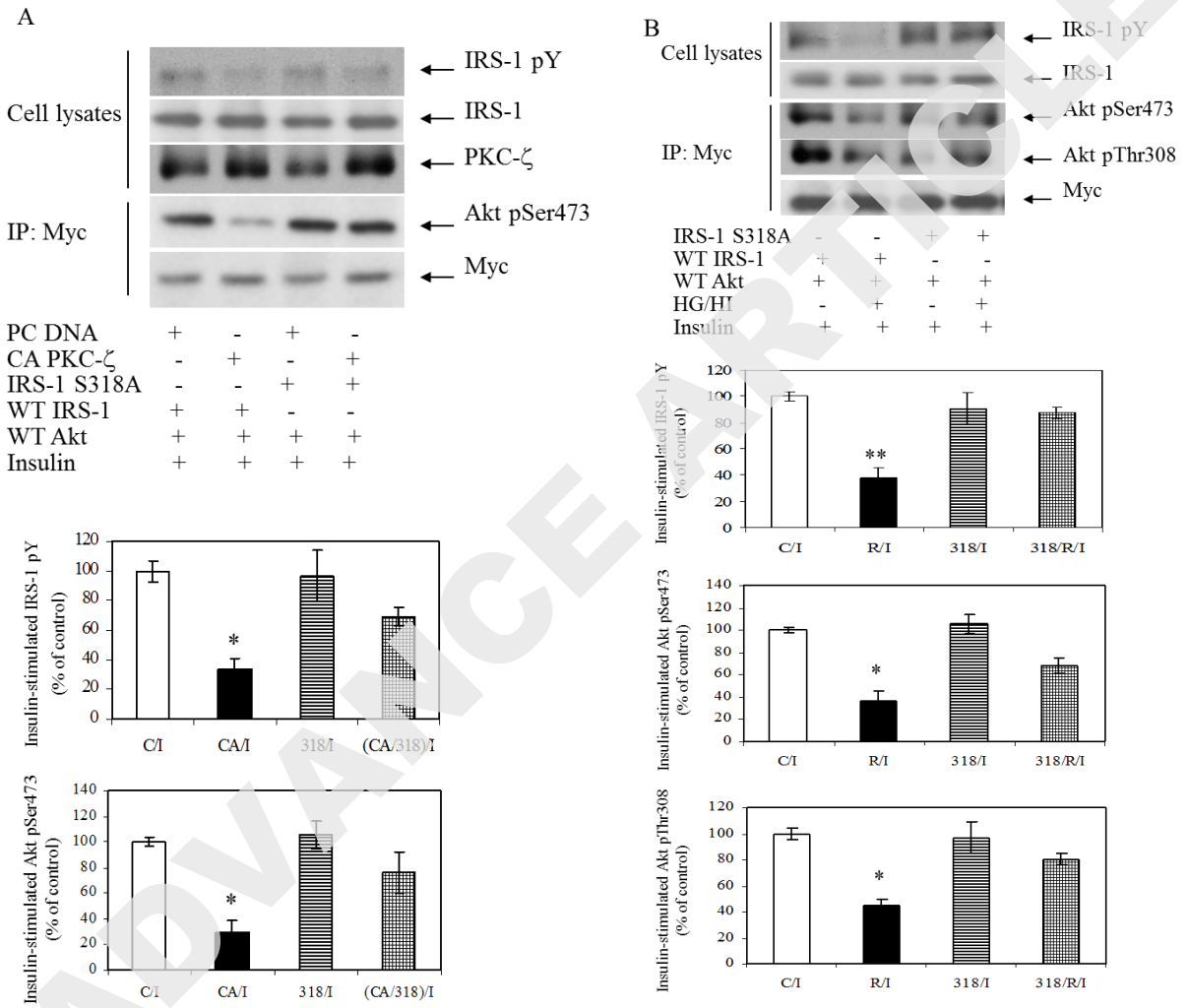

Fig. 8

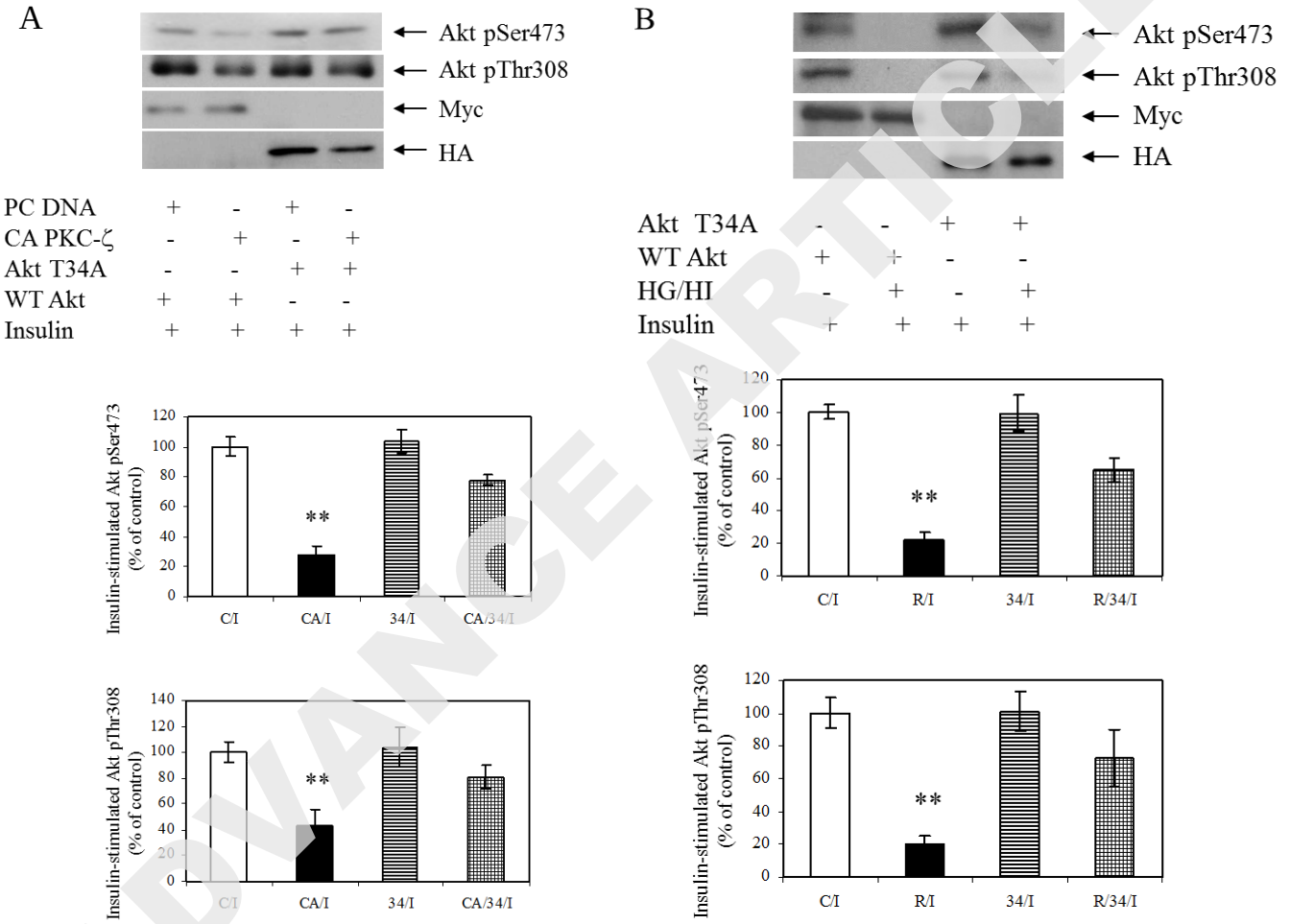

Fig. 9

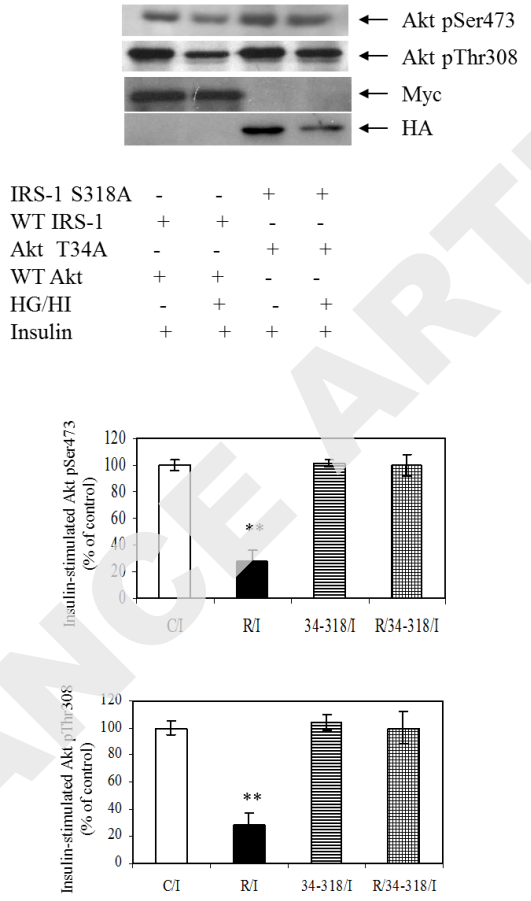

Fig. 10

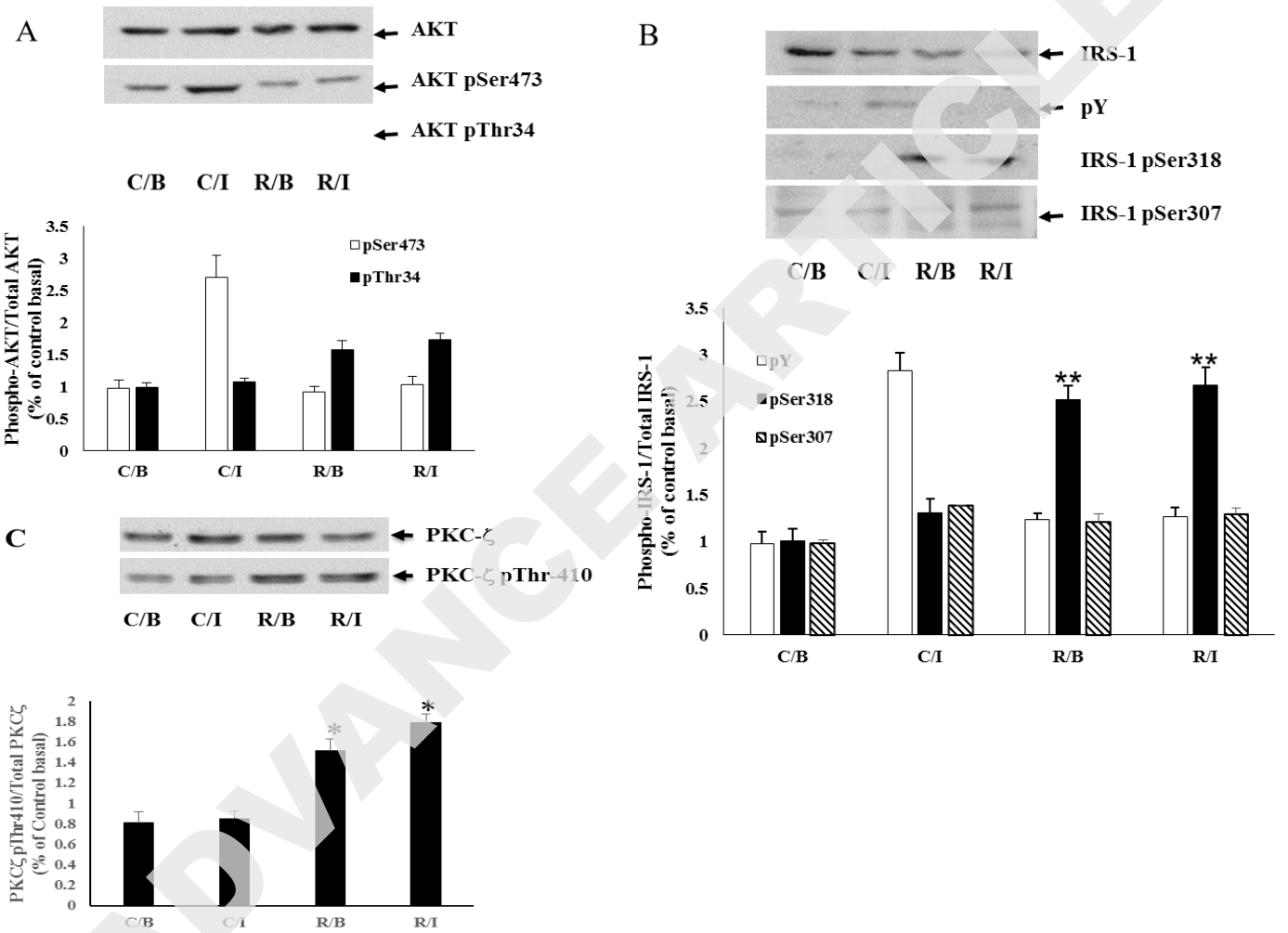

Fig. 11

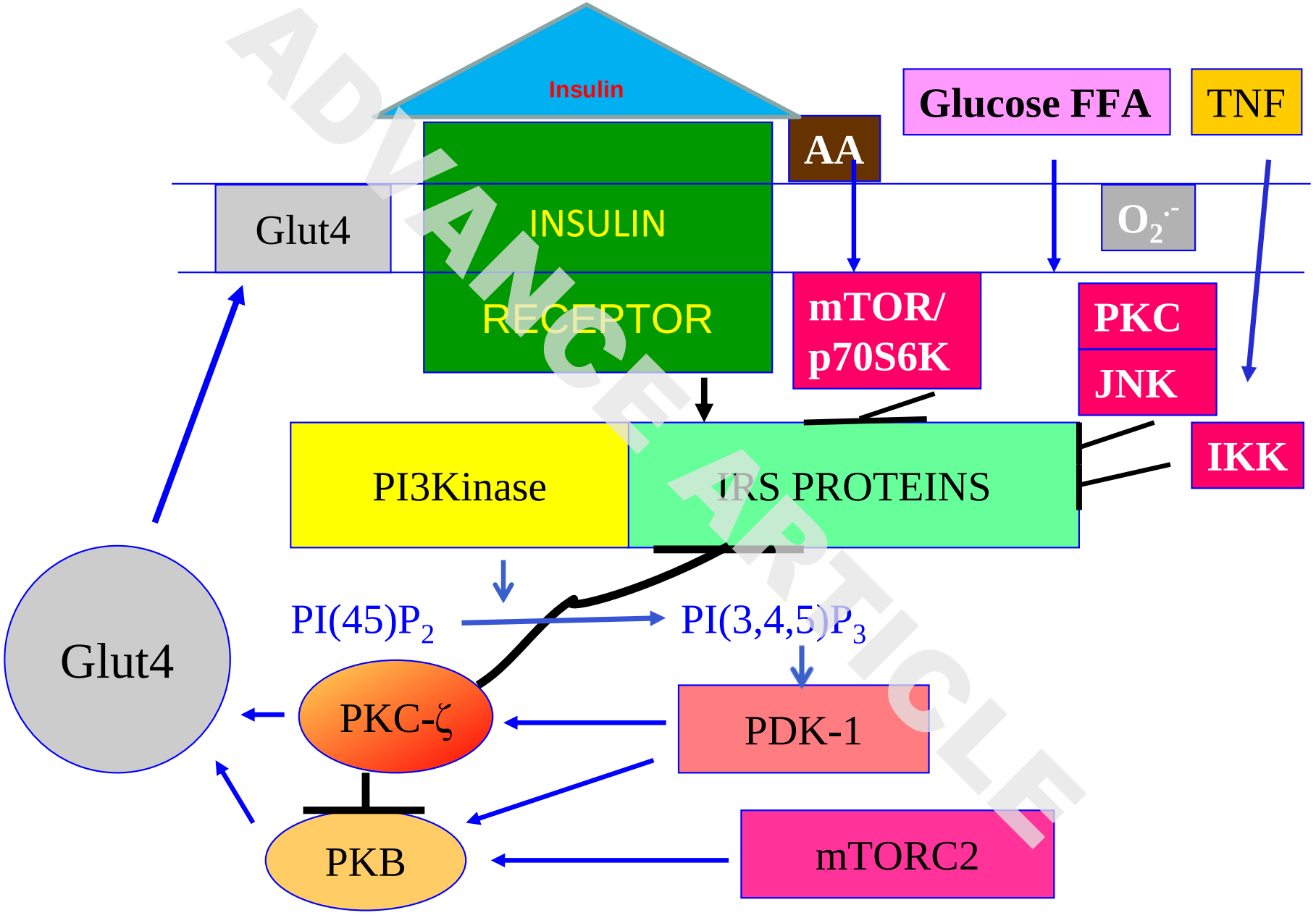

Fig. 12